GENETICS, 2023, 00(0), iyad038
https://doi.org/10.1093/genetics/iyad038
Advance Access Publication Date: 13 March 2023
Investigation

Distinct *Wolbachia* localization patterns in oocytes of diverse host species reveal multiple strategies of maternal transmission

Yonah A. Radousky,[1,‡] Michael T. J. Hague,[2,*,‡] Sommer Fowler,[1] Eliza Paneru,[1] Adan Codina,[1] Cecilia Rugamas,[1] Grant Hartzog,[1] Brandon S. Cooper,[2] William Sullivan[1]

[1]Department of Molecular, Cell, and Developmental Biology, University of California Santa Cruz, Santa Cruz, CA 95064, USA
[2]Division of Biological Sciences, University of Montana, Missoula, MT 59812, USA

*Corresponding author: Division of Biological Sciences, University of Montana, 32 Campus Dr. HS 104, Missoula, MT 59812, USA. Email: michael.hague@mso.umt.edu
‡Co-first authors.

Abstract

A broad array of endosymbionts radiate through host populations via vertical transmission, yet much remains unknown concerning the cellular basis, diversity, and routes underlying this transmission strategy. Here, we address these issues, by examining the cellular distributions of *Wolbachia* strains that diverged up to 50 million years ago in the oocytes of 18 divergent *Drosophila* species. This analysis revealed 3 *Wolbachia* distribution patterns: (1) a tight clustering at the posterior pole plasm (the site of germline formation); (2) a concentration at the posterior pole plasm, but with a significant bacteria population distributed throughout the oocyte; and (3) a distribution throughout the oocyte, with none or very few located at the posterior pole plasm. Examination of this latter class indicates *Wolbachia* accesses the posterior pole plasm during the interval between late oogenesis and the blastoderm formation. We also find that 1 *Wolbachia* strain in this class concentrates in the posterior somatic follicle cells that encompass the pole plasm of the developing oocyte. In contrast, strains in which *Wolbachia* concentrate at the posterior pole plasm generally exhibit no or few *Wolbachia* in the follicle cells associated with the pole plasm. Taken together, these studies suggest that for some *Drosophila* species, *Wolbachia* invade the germline from neighboring somatic follicle cells. Phylogenomic analysis indicates that closely related *Wolbachia* strains tend to exhibit similar patterns of posterior localization, suggesting that specific localization strategies are a function of *Wolbachia*-associated factors. Previous studies revealed that endosymbionts rely on *1* of 2 distinct routes of vertical transmission: continuous maintenance in the germline (germline-to-germline) or a more circuitous route via the soma (germline-to-soma-to-germline). Here, we provide compelling evidence that *Wolbachia* strains infecting *Drosophila* species maintain the diverse arrays of cellular mechanisms necessary for *both* of these distinct transmission routes. This characteristic may account for its ability to infect and spread globally through a vast range of host insect species.

Keywords: *Wolbachia*, *w*Mel, host–microbe interactions, vertical transmission, *Drosophila*

Introduction

A large class of endosymbionts rely on efficient vertical transmission to ensure their maintenance and spread through host populations. Many insect endosymbionts achieve this by a strict association with the host germline through successive generations. That is, during oogenesis, endosymbionts target the extreme posterior of the oocyte, the site of germline formation. In contrast to this strict germline-to-germline route of maternal transmission, other endosymbionts occupy the germline via invasion from neighboring somatic cells (Russell *et al.* 2019). Occupation of the germline via a somatic route requires that the endosymbiont has the capacity to undergo cell-to-cell transmission.

Among all known endosymbionts, maternally transmitted *Wolbachia pipientis* is the most common, infecting 30–60% of all insect species (Hilgenboecker *et al.* 2008; Zug and Hammerstein 2012; Weinert *et al.* 2015). Hosts acquire *Wolbachia* from other species via horizontal (non-sexual) transfer or from sister species via introgressive transfer (O'Neill *et al.* 1992; Raychoudhury *et al.* 2009; Gerth and Bleidorn 2016; Conner *et al.* 2017; Turelli *et al.* 2018; Cooper *et al.* 2019). Following establishment, maternal transmission rates in conjunction with *Wolbachia* effects on host fitness and reproduction determine *Wolbachia* spread and prevalence in host populations (Hoffmann *et al.* 1990; Turelli and Hoffmann 1995; Cooper *et al.* 2017; Cogni *et al.* 2021).

While sometimes imperfect, the success and prevalence of *Wolbachia* ultimately depend on vertical transmission through the female (Hoffmann *et al.* 1990; Turelli and Hoffmann 1995; Carrington *et al.* 2011; Hague *et al.* 2022). The ability of *Wolbachia* to establish and persist in diverse insect species indicates that it has evolved to usurp highly conserved host processes and components. For example, studies of *w*Mel *Wolbachia* in model organism *Drosophila melanogaster* suggest that *Wolbachia* engage conserved

Received: November 28, 2022. **Accepted:** February 21, 2023

host motor proteins dynein and kinesin in order to target the extreme posterior of the oocyte, the site of germline formation (Ferree *et al.* 2005; Serbus and Sullivan 2007; Russell *et al.* 2018).

To study the vertical transmission of *Wolbachia* in *Drosophila*, we take advantage of the wealth of knowledge regarding the molecular and cell biology of *Drosophila* oogenesis (for a review, see Bastock and St Johnston 2008). *Drosophila* ovaries contain 2 clusters of ovarioles, each containing 2–3 germline stem cells and various stages of developing oocytes. The stem cells undergo asymmetric mitotic division in which 1 daughter cell undergoes self-renewal and the other differentiates into a cytoblast. The cytoblast undergoes 4 rounds of mitotic divisions resulting in 16 interconnected cells, 1 of which becomes the oocyte nucleus while the others differentiate into polyploid nurse cells. The developing oocyte is encapsulated by a monolayer of somatically derived follicle cells resulting in the formation of discrete egg chambers as the maturing oocyte progresses through the ovariole. During the late stages of oogenesis, the nurse cell cytoplasm is expelled into the oocyte, resulting in a rapid doubling of the oocyte volume and concomitant shrinking of nurse cell volume (Theurkauf and Hazelrigg 1998; Bastock and St Johnston 2008). This is followed by posterior pole plasm formation and establishment of the germline (Bilinski *et al.* 2017).

Wolbachia distribution and localization in insect oocytes and early embryos have been well characterized in *w*Mel-infected *D. melanogaster* (Kose and Karr 1995; Veneti *et al.* 2004; Ferree *et al.* 2005; Serbus *et al.* 2008; Ramalho *et al.* 2018; Russell *et al.* 2018; Guo *et al.* 2019). Early in oogenesis, *w*Mel *Wolbachia* are evenly distributed throughout all the cells in the chamber. At this stage, microtubules emanate from the oocyte into the nurse cells (Theurkauf 1994; Grieder *et al.* 2000). By associating with the minus-end–directed microtubule motor protein dynein, *w*Mel *Wolbachia* are transported from the nurse cells and concentrate at the anterior end of the oocyte (Ferree *et al.* 2005). As the oocyte matures, microtubules undergo a dramatic reorganization such that they originate from the oocyte cortex with their plus-ends oriented toward the posterior pole (Theurkauf *et al.* 1992; Steinhauer and Kalderon 2006). This reorganization is accompanied by a release and dispersal of *w*Mel *Wolbachia* from the anterior pole. Then, *w*Mel *Wolbachia* associate with the plus-end–directed motor protein kinesin for transport to the posterior pole and the site of germline formation (Serbus and Sullivan 2007). There, *Wolbachia* (*w*Mel) associate with pole plasm determinants maintaining their position at the site of germline formation (Serbus and Sullivan 2007) in spite of extensive cytoplasmic streaming (Serbus *et al.* 2005).

Thus, *w*Mel *Wolbachia* location and migration patterns provide insights into the host factors with which *Wolbachia* engages throughout oogenesis. The *Drosophila simulans*-associated *w*Ri strain exhibits a similar anterior distribution in early oogenesis and then becomes distributed across the entire mature oocyte. However, unlike *w*Mel, it does not concentrate at the posterior pole of the oocyte (Veneti *et al.* 2004; Serbus and Sullivan 2007). This suggests *w*Ri engages host dynein and kinesin, but not pole plasm determinants. *w*Mel *Wolbachia* strains introgressed into a *D. simulans* host background exhibit a concentration in the pole plasm, indicating the *Wolbachia* genome rather than the host genome drives oocyte localization properties (Poinsot *et al.* 1998; Veneti *et al.* 2004; Serbus and Sullivan 2007).

With the exception of *w*Mel and *w*Ri, little is known of the extent to which distribution patterns in the oocyte and transmission routes vary among diverse *Wolbachia* strains and host species. Here, we fill this important knowledge gap, by examining 18 *Drosophila* host species infected with *Wolbachia* strains that diverged up to 50 million years ago. These studies also provide a direct read-out of *Wolbachia* and host motor protein–pole plasm interactions that are highly conserved and those that vary among species. This work complements and extends previous analyses revealing *Wolbachia* strain-dependent localization patterns in the *Drosophila* oocyte and embryo (Veneti *et al.* 2004; Toomey *et al.* 2013).

We discovered that *Wolbachia* distribution patterns in the *Drosophila* oocytes fall into 3 categories: (1) the vast majority of *Wolbachia* clusters at the posterior pole; (2) a concentration at the posterior pole, but with a large portion of *Wolbachia* distributed throughout the entire oocyte; and (3) *Wolbachia* distributed throughout the oocyte, with none or very few located at the posterior pole. This latter class is particularly interesting as it suggests *Wolbachia* likely enters the oocyte via a somatic route for transmission to the next generation. We also provide evidence that neighboring somatic follicle cells are the likely source of *Wolbachia* entering the germline. Together, these findings indicate that *Wolbachia* are capable of achieving efficient vertical transmission either via strict maintenance in the germline from 1 generation to the next or via invasion of the germline through neighboring somatic cells. Thus, *Wolbachia* must maintain the diverse arrays of cellular mechanisms necessary for *both* of these distinct transmission routes. We identify candidate surface proteins that may be responsible for these diverse localization patterns in host oocytes.

Materials and methods

Drosophila stocks

All stocks were grown on standard brown food (Sullivan *et al.* 2000) at 25°C with a 12-h light/dark cycle. Uninfected *Drosophila* stocks were generated by tetracycline curing of the infected stock (Serbus *et al.* 2015). Listed in Table 1 are the 19 different *Wolbachia* strains we examined, which infect 18 different *Drosophila* host species. This included 6 *w*Mel-like strains (Cooper *et al.* 2019; Hague *et al.* 2020a), 5 *w*Ri-like strains (Turelli *et al.* 2018), 7 other A-group *Wolbachia*, and the B-group strain *w*Mau that diverged from A-group *Wolbachia* up to 46 million years ago (Meany *et al.* 2019). Each genotype was generated as an isofemale line by sampling a single gravid female from the field and placing her individually into a vial.

Ovary, embryo, and larva fixation and staining

Newly eclosed flies were transferred to fresh food for 3–5 days for aging. Approximately 10 females were dissected for each slide preparation. Ovaries were fixed using a modification of previously published procedures (Brendza *et al.* 2000; Russell *et al.* 2018). Ovaries were removed and separated in phosphate buffer solution and then fixed in a 200-µl devitellinizing solution (2% paraformaldehyde and 0.5% v/v NP40 in 1× PBS) mixed with 600 µl heptane for 20 min at room temperature, on a shaker. After removal of the organic layer by brief centrifugation for sample isolation, the ovaries were washed 3 times with PBS-T (0.1% Triton X-100 in 1× PBS) along with three 5-min washes. Samples were treated with RNAse A (10 mg/ml) and left overnight at room temperature. Samples were then washed again a few times with PBS-T and then stained with a dilute solution of phalloidin for actin staining on a rotator for 1 h. Samples were washed again with 3 quick PBS-T rounds and then solution changes with PBS-T over 2 h. Sixty microliters of propidium iodide (PI) in mounting media was added to the sample after removal of the wash solution and left again

Table 1. Qualitative and quantitative quantification of cellular *Wolbachia* abundance in stage 10 oocytes.

Wolbachia strain	Host species	Localization class	N	Whole oocyte mean CTCF	Posterior mean CTCF	Posterior cortex mean CTCF
*w*Rec	*D. recens*	Clumped	3	482,174	300,753	58,453
*w*Tris	*D. tristis*	Localized	4	223,048	129,013	105,641
*w*Seg	*D. seguyi*	Dispersed	5	58,552	11,402	557
*w*Cha	*D. chauvacae*	Localized	5	108,588	42,636	9,786
*w*Burl	*D. burlai*	Localized	4	72,806	53,754	36,944
*w*Mel	*D. melanogaster*	Localized	2	191,451	136,174	92,341
*w*Bic	*D. bicornuta*	Clumped	3	90,114	83,621	54,900
*w*Ri	*D. simulans*	Dispersed	5	333,505	90,664	20,494
*w*Pan	*D. pandora*	Localized	3	45,423	6,486	1,890
*w*Ana	*D. ananassae*	Localized	4	41,578	16,843	12,927
*w*Tria	*D. triauraria*	Dispersed	2	487,897	1,809	345
*w*Aura	*D. auraria*	Dispersed	5	266,478	3,699	645
*w*Ha	*D. simulans*	Dispersed	5	82,941	3,488	807
*w*Bai	*D. baimaii*	Dispersed	2	11,359	0	0
*w*Boc	*D. bocki*	Clumped	6	137,664	98,339	82,408
*w*Leo	*D. leontia*	Clumped	4	997,045	685,260	713,918
*w*Tsa	*D. tsacasi*	Localized	4	61,314	36,478	20,620
*w*Nik	*D. nikananu*	Localized	3	44,764	27,099	13,014
*w*Mau	*D. mauritiana*	Dispersed	3	69,362	799	322

The number of confocal images (*N*) used to generate means is shown for each *Wolbachia*-infected host species. *Wolbachia* abundance was measured in each region of the oocyte as corrected total cell fluorescence (CTCF).

overnight. Ovaries were then mounted and carefully separated out again for ease of imaging and removal of excess mature eggs. Slides were coated in nail polish and stored at −20°C until imaged.

Embryos were collected for 1–3 h on plates and fixed in equal volume 32% paraformaldehyde and heptane and fixed as previously described (Sullivan *et al.* 2000). After extraction with methanol, embryos were blocked for 1 h in 5% PBST–BSA (2.5 g bovine serum albumin fraction V in 50 ml PBS-T) at room temperature. Embryos were then incubated with anti-WD_0009 or anti-FtsZ at 1:500 overnight at 4°C. After 3 washes with 1% PBST–BSA over 1 h, embryos were incubated in Alexa 488 Anti-Rabbit at 1:500 for 1 h at room temperature. Samples were then washed 3 more times over 1 h with 1% PBST–BSA. Embryos were mounted with media containing DAPI and stored at −20°C until imaged.

Larval fat bodies were dissected and fixed from the 3rd instar larvae using a modified version of a published protocol (Maimon and Gilboa 2011). Fat bodies were dissected in 1× PBS then fixed in 5% paraformaldehyde in PBS for 20 min with gentle agitation. Fat bodies were washed for 5 min, 10 min, then 45 min with cold 1% NP40 in PBS. After washes, fat bodies were blocked in 5% PBST–BSA (2.5 g bovine serum albumin fraction V in 50 ml PBS-T) for 1 h at room temperature. Fat bodies were then incubated with anti-FtsZ at 1:500 overnight on a rocker at 4°C, washed 3 times over 1 h with 1% PBST–BSA, and then incubated with Alexa 488 Anti-Rabbit at 1:500 at room temperature for 1 h. After 3 additional washes over 1 h with 1% PBST–BSA, fat bodies were mounted onto a slide with media containing DAPI. Larval ovaries were isolated from fat bodies using 0.1-mm needles before sealing the slide with nail polish. Samples were then stored at −20°C.

Confocal microscopy

Imaging was performed on an inverted Leica DMI6000 SP5 scanning confocal microscope. Optical sections of a Nyquist value of 0.38 were used. A variety of zooms were used to optimize image viewing, with most being set at 1.5×. Propidium iodide was excited with the 514- and 543-nm lasers, and emission from 550 to 680 nm was collected. GFP was imaged with the 488-nm laser, and emission from 488 to 540 nm was collected. Alexa 633 was imaged with the 633 laser, and emission from 606 to 700 nm was collected. All imaging was performed at room temperature. Images were acquired with Leica Application Suite Advanced Fluorescence software.

Wolbachia quantification and analysis

Following Russell *et al.* (2018), we used the polygon selection tool to select 3 different regions of the oocyte (see Supplementary Fig. 1 in Russell *et al.* 2018): the whole oocyte, the posterior region, and the posterior cortex. The "area" and "integrated density" were measured for each region. Additionally, the average of a quadruplicate measure of "mean gray value" beside the stained oocytes was measured as background fluorescence. The corrected total cell fluorescence (CTCF) was calculated as integrated density − (area × background mean gray value) for each region.

All statistical analyses were performed in R. We first tested whether our 3 qualitative classes (posteriorly clumped, posteriorly localized, and dispersed) differed significantly in quantitative estimates of *Wolbachia* fluorescence (CTCF). We used a one-way ANOVA to test if the 3 groups differed based on their mean CTCF values from the whole oocyte, the posterior region, and the posterior cortex. Distribution and leverage analyses indicated that a transformation of $x' = \log(x+1)$ was needed to meet assumptions of normality. We tested for significance using an *F* test with type III sum of squares using the "Anova" function in the *car* package (Fox and Weisberg 2019). We conducted Tukey's multiple comparisons among the 3 groups using the "TukeyHSD" function.

Genomic data

In order to perform the phylogenomic analysis and generate phylograms, we obtained *Wolbachia* sequences from publicly available genome assemblies, which included *w*Mel (Wu *et al.* 2004), *w*Ri (Klasson *et al.* 2009), *w*Ha (Ellegaard *et al.* 2013), *w*Aura, *w*Tria, *w*Pan (Turelli *et al.* 2018), *w*Ana (Salzberg *et al.* 2005), and *w*Rec (Metcalf *et al.* 2014). All other *Wolbachia* sequences included in this study [*w*Bai, *w*Bic, *w*Boc, *w*Burl, *w*Cha, *w*Curt (*w*Tsa), *w*Nik, *w*Seg, *w*Tris, and *w*Leo] were obtained using Illumina sequencing and previously described methods (Hague *et al.* 2020b). Briefly, tissue samples for genomic data were extracted using a DNeasy Blood & Tissue kit (Qiagen). DNA was cleaned using Agencourt AMPure XP beads (Beckman Coulter, Inc.)

following manufacturers' instructions and eluted in 50 μl 1 × TE buffer for shearing. DNA was sheared using an E220 Focused Ultrasonicator (Covaris Inc.) to a target size of 400 bp. We prepared libraries using NEBNext Ultra II DNA Library Prep with Sample Purification Beads (New England BioLabs). We indexed samples using NEBNext Multiplex Oligos for Illumina (Index Primers Set 3 and Index Primers Set 4), and 10 μl of each sample was shipped to Novogene (Sacramento, CA, USA) for sequencing using Illumina HiSeq 4000, generating paired-end 150 bp reads.

We obtained publicly available host sequences for *D. melanogaster* (Hoskins *et al.* 2015), *D. simulans* (Hu *et al.* 2013), *Drosophila ananassae* (Clark *et al.* 2007), *Drosophila pandora* (Turelli *et al.* 2018), *Drosophila mauritiana* (Meany *et al.* 2019), *Drosophila auraria*, *Drosophila triauraria*, *Drosophila baimaii*, *Drosophila bicornuta* (aff. *bicornuta*), *Drosophila bocki*, *Drosophila burlai*, *Drosophila chauvacae* (cf. *chauvacae*), *Drosophila curta* (aff. *tsacasi*), *Drosophila nikananu*, *Drosophila seguyi*, *Drosophila tristis*, and *Drosophila leontia* (Conner 2021). A *Drosophila recens* genome assembly was kindly provided by Kelly Dyer and Rob Unckless. We note that 3 of the *montium* host species listed above have had recent updates to their taxonomic nomenclature: *D. bicornuta* has been renamed to aff. *bicornuta*, *chauvacae* has been renamed to cf. *chauvacae*, and *curta* has been renamed to aff. *tsacasi*. See Conner *et al.* (2021) for a full discussion of *montium* species names and relationships.

Wolbachia phylogenetic analysis

Raw Illumina reads from the newly sequenced *Wolbachia* strains were trimmed using Sickle version 1.33 (Joshi and Fass 2011) and assembled using AbySS version 2.0.2 (Jackman *et al.* 2017). *K*-values of 71, 81, and 91 were used, and scaffolds with the best nucleotide BLAST matches to known *Wolbachia* sequences with *E*-values less than 10^{-10} were extracted as the draft *Wolbachia* assemblies. For each strain, we chose the assembly with the highest N_{50} and the fewest scaffolds (Supplementary Table 1). The newly assembled genomes and the previously published assemblies were annotated using Prokka version 1.11, which identifies homologs to known bacterial genes (Seemann 2014). To avoid pseudogenes and paralogs, we only used genes present in a single copy with no alignment gaps in all of the genome sequences. Genes were identified as single copy if they uniquely matched a bacterial reference gene identified by Prokka. By requiring all homologs to have identical length in all of the *Wolbachia* genomes, we removed all loci with indels. A total of 66 genes totaling 43,275 bp met these criteria. We then estimated a Bayesian phylogram using RevBayes 1.0.8 under the GTR + Γ + I model partitioned by codon position (Höhna *et al.* 2016). Four independent runs were performed, which all converged on the same topology. All nodes were supported with Bayesian posterior probabilities of 1.

Similar methods were used to generate gene trees for candidate *Wolbachia* loci putatively involved in host interactions during oogenesis. This included the 3 *wsp* paralogs [WD_1063 (*wsp*/RS04815), WD_0009 (*wspB*/RS00060), and WD_0489 (*wspC*/RS06475)] and 3 other *Wolbachia* surface proteins [WD_1085 (bamA/RS04910), WD_0501 (p44/MSP2/RS0225), and WD_1041 (peptidase M2/RS04710)]. Here, the WD_XXXX locus tags refer to the *w*Mel genome assembly (Wu *et al.* 2004). The protein-coding sequences for each locus were extracted from the assemblies using BLAST and the *w*Mel reference sequences. Notably, we found evidence of insertions in the WD_0009 (*wspB*) sequences of *w*Boc, *w*Leo, and *w*Bic (see *Results*). We removed these large insertions from the alignment to generate the *wspB* gene tree. In addition, BLAST identified WD_0489 (*wspC*) in *w*Mel-like *Wolbachia* and closely related *w*Bai, *w*Leo, and *w*Boc, but yielded no hits in the other *Wolbachia* strains (*w*Nik, *w*Tsa, *w*Pan, *w*Ana, *w*Tria, *w*Aura, *w*Ri, and *w*Mau), indicating that *wspC* is either too diverged from the *w*Mel reference for BLAST recognition or alternatively *wspC* is only present in *w*Mel-related *Wolbachia* strains. Sequences for each gene were aligned with MAFFT 7 (Katoh and Standley 2013). We then used RevBayes and the GTR + Γ + I model partitioned by codon position to generate gene trees for each locus.

Host phylogenetic analysis

Host phylogenies were generated using the same nuclear genes implemented in Turelli *et al.* (2018): *aconitase*, *aldolase*, *bicoid*, *ebony*, *enolase*, *esc*, *g6pdh*, *glyp*, *glys*, *ninaE*, *pepck*, *pgi*, *pgm*, *pic*, *ptc*, *tpi*, *transaldolase*, *white*, *wingless*, and *yellow*. We used BLAST with the *D. melanogaster* coding sequences to extract orthologs from the genomes of each host species. Sequences were then aligned with MAFFT 7. Finally, we used RevBayes and the GTR + Γ + I model partitioned by codon position and gene to accommodate potential variation in the substitution process among genes, as described in Turelli *et al.* (2018). Our initial phylogenetic analysis produced a polytomy in the *melanogaster* species group regarding the relationships among the *montium*, *melanogaster*, and *ananassae* subgroups (Supplementary Fig. 1). These relationships have been resolved in previous genomic studies involving additional taxa (Turelli *et al.* 2018; Suvorov *et al.* 2022); therefore, we generated a constrained host tree in RevBayes that enforced previously defined relationships among the 3 subgroups: [(*montium*, *melanogaster*) and *ananassae*].

Tests for phylogenetic signal

The resulting phylograms were used to test whether cellular *Wolbachia* abundance in oocytes exhibits phylogenetic signal on either the *Wolbachia* or host phylogenies. We used our quantitative estimates of *Wolbachia* abundance to test for phylogenetic signal using Pagel's lambda (λ) (Pagel 1999). Here, we used total *Wolbachia* fluorescence in whole oocytes, the posterior region, and the posterior cortex (log-transformed CTCF) as continuous characters to calculate maximum likelihood values of Pagel's λ. A Pagel's λ of 0 indicates that character evolution occurs independently of phylogenetic relationships, whereas λ = 1 is consistent with a Brownian motion model of character evolution. We used the "fitContinuous" function in GEIGER (Harmon *et al.* 2008) and a likelihood ratio test to compare our fitted value to a model assuming no phylogenetic signal (λ = 0). We also used a Monte Carlo-based method to generate 95% confidence intervals surrounding our estimates using 1,000 bootstrap replicates in the *pmc* package (Boettiger *et al.* 2012). When applicable, we conducted additional analyses to evaluate whether the number of taxa in our phylogeny ($N = 19$ *Wolbachia* strains and $N = 18$ host species) limited our ability to detect significant departures from λ = 0 (Hague *et al.* 2020b, 2021). Small phylogenies are likely to generate near 0 values simply by chance, not necessarily because the phylogeny is unimportant for trait evolution (Boettiger *et al.* 2012). To evaluate whether larger phylogenies increase the accuracy of estimation, we simulated trees with an increasing number of *Wolbachia* strains/host species ($N = 25$ and 50) and our empirical estimates using the "sim.bdtree" and "sim.char" functions in the *geiger* R package (Harmon *et al.* 2008). We then re-estimated confidence intervals using the larger simulated trees.

Our tests for phylogenetic signal using the constrained host phylogram are presented in the main text; however, we note that our analysis using the unconstrained host tree (with a

polytomy at the base of the *melanogaster* species group) produced similar results. Using the unconstrained tree, we found that *Wolbachia* abundance in whole oocytes [$\lambda = 0.782$ (0, 0.987), $P = 0.469$], the posterior region [$\lambda = 0.951$ (0, 1), $P = 0.377$], and the posterior cortex [$\lambda < 0.001$ (0, 0.563), $P = 1$] did not exhibit significant phylogenetic signal.

Structural analysis of *Wolbachia* candidate genes

We used HHPred to identify protein domains of WD_1085 and WD_0501 using the COPe70_2.07, Pfam-A_v33.1, COG_KOG_v1.0, and SMART_v6 databases (Zimmermann *et al.* 2018; Gabler *et al.* 2020). Here, we used default setting, including an *E*-value cutoff for MSA generation of 1e−3, a minimum coverage of MSA hits of 20%, a minimum probability in hitlist of 20%, and a maximum of 250 target hits. As expected, both WD_1085 and WD_0501 yielded multiple hits of varying length for domains associated with outer membrane proteins that form beta barrel structures (results summarized in Supplementary Table 2). We used SignalP-6.0 to identify the signal peptide cleavage sites for WD_1085 between aa residues 25 and 26 (Teufel *et al.* 2022) and removed the signal peptide for homology modeling. SignalP was unable to confidently identify the signal peptide sequence for WD_0501, so we used the full sequence for homology modeling. We then used I-TASSER to model the 3D structure of each protein through sequence homology (Yang and Zhang 2015; Zhang *et al.* 2017). For WD_1085, we used PDB:4K3B with an amino acid sequence identity of 23% in the threaded aligned region as a template (Noinaj *et al.* 2103). For WD_0501, we used PDB:2MLH with an amino acid sequence identity of 17% in the threaded aligned region as a template (Fox *et al.* 2014). PyMOL was used for image generation (Schrodinger 2015). Results are displayed in Supplementary Fig. 2.

Ectopic expression of *Wolbachia* surface proteins in yeast

SC–leucine yeast media was prepared as described previously (Ros *et al.* 1990). Where present, benomyl was added to media from a 10 mg/ml stock in DMSO to a final concentration of 2.5 µg/ml. The yeast expression assays are a modified version of the protocol described by Sheehan *et al.* (2016). *Wolbachia* genes were codon optimized for expression in *Saccharomyces cerevisiae* and synthesized by Twist Bioscience (South San Francisco). The *wsp*, *wspB*, and *wspC* genes were gifts of the Free Genes Project (https://stanford.freegenes.org/). These genes were inserted into pGH448 using the New England Biolabs Golden Gate kit according to the manufacturer's instruction. This placed the *Wolbachia* genes under control of the *GAL1* promoter and *CYC1* transcriptional terminator. This plasmid, which will be described in more detail elsewhere, carries a CEN/ARS element and also contains the kanamycin resistance and *LEU2* genes for selection in bacteria and yeast, respectively.

The indicated plasmids were transformed into yeast strain GHY1934 (*MAT***a** *his3Δ200 lys2-128δ leu2Δ1 ura3-52 trp1Δ63 pGAL1-FLO8-HIS3::KANMX*) and GHY1551 (*MATα his3Δ1 leu2Δ0 lys2Δ0 ura3Δ0 mad1Δ::KANMX*). Both of these strains are isogenic to S288C and are *GAL2+*. Transformed cells were grown to saturation in SC–leucine liquid media containing 2% glucose. These cells were counted, diluted to 1×10^{-7} cells per ml, 5-fold serial diluted, and spotted to SC–leucine plates with either 2% glucose or 2% galactose as the carbon source and incubated at the times and temperatures indicated in the figure legends.

Results

Wolbachia navigates the developing *Drosophila* oocyte in distinct stages

As described above, *w*Mel *Wolbachia* migration and distribution throughout oogenesis in *D. melanogaster* have been well documented (Kose and Karr 1995; Veneti *et al.* 2004; Serbus and Sullivan 2007; Serbus *et al.* 2008; Ramalho *et al.* 2018; Russell *et al.* 2018; Guo *et al.* 2019). As a reference for our analysis of *Wolbachia* oocyte distributions in a range of *Drosophila* species, the key distribution patterns of *w*Mel throughout *D. melanogaster* oocytes are depicted in Fig. 1.

Stage 1 includes the germarium, a structure consisting of the germline stem cells and their cystoblast daughter cells that will differentiate into mature oocytes. Progression to stage 2 involves the cystoblast undergoing 4 rounds of mitotic division to produce a syncytium of 16 cells connected by cytoplasmic bridges and surrounded by a layer of somatically derived follicle cells (Bastock and St Johnston 2008). Propidium iodide (PI)-stained *Wolbachia* (red) are clearly observed as puncta in the cytoplasm of the infected, but not the uninfected 16 cell cyst (Fig. 1, stages 1 and 2, arrows). Actin is labeled in green.

During stage 3, the cyst has become polarized with 1 of the cells differentiating into an oocyte and the others becoming polyploid nurse cells. At this stage, *Wolbachia* rely on dynein-mediated microtubule transport (Ferree *et al.* 2005) and are clearly seen in the infected oocyte cytoplasm anteriorly concentrated at 2 cytoplasmic bridges that connect to the nurse cells (Fig. 1, stage 3, arrows).

During stages 4 and 5, the nurse cell–oocyte complex becomes oblong and is fully encapsulated by follicle cells. *Wolbachia* are clearly observed in both the oocyte and nurse cell cytoplasm (Fig. 1, stages 4 and 5, arrows). The *Wolbachia* in the oocyte are tightly associated with the anterior cortex.

During stage 6, the number of follicle cells increases and they are more densely packed in a monolayer encompassing the oocyte. Here, we discovered a previously unrecognized aspect of *Wolbachia* dynamics and localization: the number of anteriorly localized *Wolbachia* is greatly diminished at this stage (Fig. 1, stage 6, arrow). This pattern was consistent across all 10 of the stage 6 oocytes we observed in our analysis (see Supplementary Fig. 3).

At stage 7, *Wolbachia* are again observed in the oocyte. However, rather than being tightly associated with the anterior cortex, *Wolbachia* are evenly distributed throughout the oocyte (Fig. 1, stage 7, arrow). During stage 7, the microtubules reorient such that their plus-ends extend toward the posterior pole (Cha *et al.* 2001, 2002; Steinhauer and Kalderon 2006). Accordingly, the plus-end motor protein kinesin is required to establish the even distribution of *Wolbachia* throughout the maturing oocyte (Serbus and Sullivan 2007). Stage 8 heralds the beginning of vitellogenesis, the process of yolk formation and deposition of nutrients into the oocyte (Cummings *et al.* 1971). *Wolbachia* are near, but not yet located at, the posterior pole (Fig. 1, stage 8, arrow). At stage 9, anterior follicle cell migration occurs (Rørth 2002). At this stage, *Wolbachia* displays an arch-like posterior cortical localization (Fig. 1, stage 9, arrow). By stage 10, there is a distinct concentration of *Wolbachia* along the posterior cortex, the site of germline formation (Fig. 1, stage 10, arrow). Nurse cell dumping will shortly follow, leading into stages 11 and 12 with the oocyte rapidly growing in size (Mahajan-Miklos and Cooley 1994).

The *w*Mel strain in *D. melanogaster* provides an outline of the molecular and cellular mechanisms driving *Wolbachia* vertical transmission. It also raises the question of whether the mechanisms and strategies observed in *D. melanogaster* are conserved

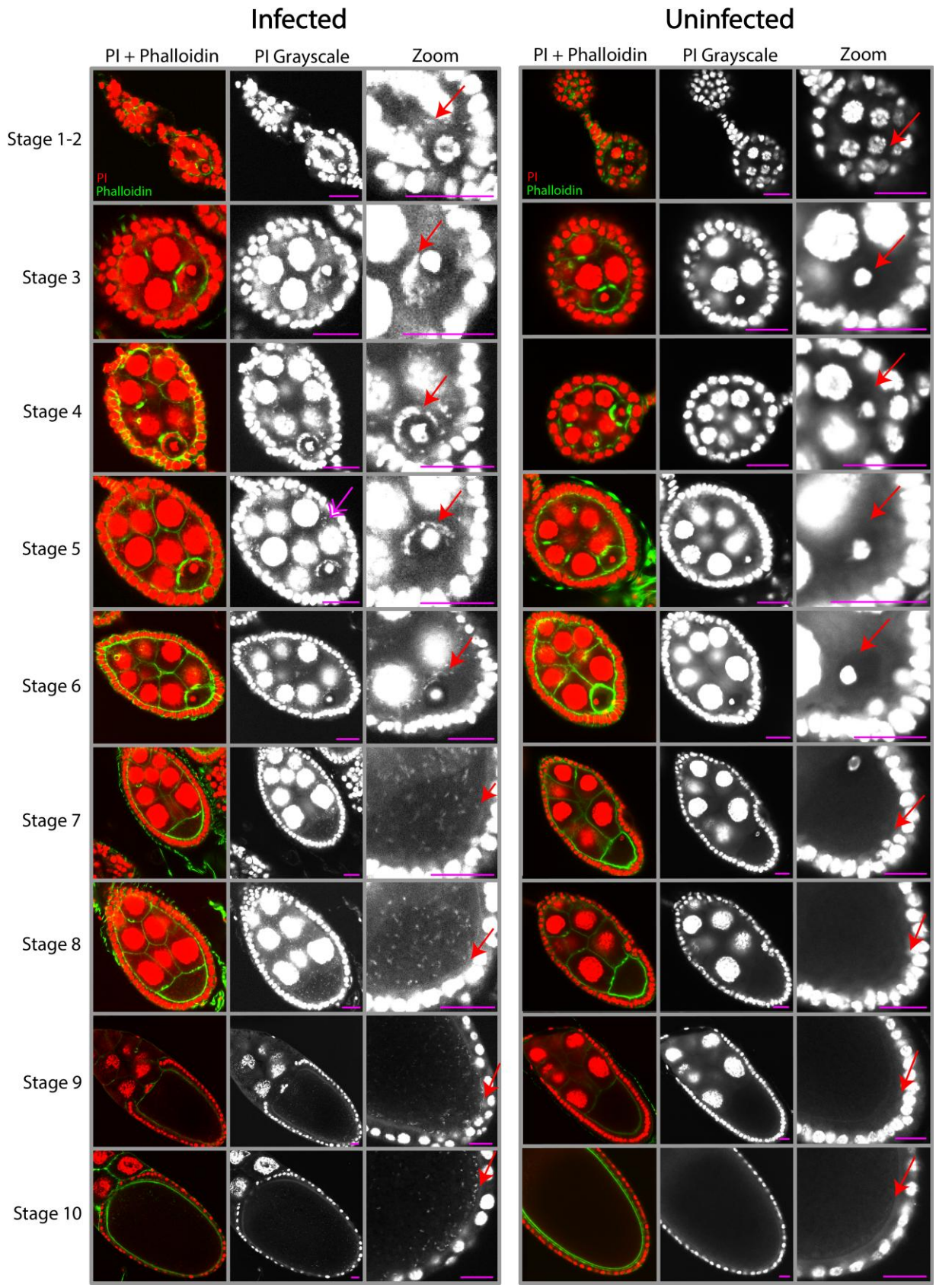

Fig. 1. Confocal micrographs of *D. melanogaster* (*w*Mel) oocytes tracked through early oogenesis. Samples are stained with propidium iodide (PI) for DNA (red) and phalloidin for actin (green). Representative stages of development (1–10) are shown for *w*Mel infected (left panels) and uninfected (right panels). Grayscale zoomed-in images around the nucleus of the oocyte are shown in the 3rd column, with red arrows highlighting *Wolbachia* in the oocyte. Corresponding arrows in the 6th column show the equivalent area in uninfected oocytes. The magenta double arrow in the stage 5 infected oocyte (2nd column) highlights *Wolbachia* in the nurse cells. Scale bars all set to 25 μM.

across diverse *Wolbachia* strains and *Drosophila* species. To explore this issue, the *w*Mel distribution in *D. melanogaster* serves as the basis for our comparison of 18 other *Wolbachia* strains. Bayesian phylograms depicting phylogenetic relationships among the *Wolbachia* strains and the *Drosophila* species are shown in Fig. 4 and Supplementary Fig. 4. Our analysis comprised 18 A-group *Wolbachia* strains, including 6 *w*Mel-like strains (Cooper *et al.* 2019; Hague *et al.* 2020a) and 5 *w*Ri-like strains (Turelli *et al.* 2018), as well as the B-group *Wolbachia* strain *w*Mau, which diverged from A-group *Wolbachia* up to 50 million years ago (Meany *et al.* 2019). These *Wolbachia* strains infect 18 divergent *Drosophila* host species spanning 3 species groups (Suvorov *et al.* 2022).

An initial concentration of *Wolbachia* at the oocyte anterior is a conserved feature

As described above, *w*Mel *Wolbachia* enter the oocyte through a complex of ring canals connecting the nurse cells to the oocyte and concentrate at the anterior cortex at stages 3–5. Initially observed in *D. melanogaster*, the number of *Wolbachia* increases dramatically while at the anterior (Ferree *et al.* 2005). To determine if anterior localization is a conserved aspect of *Wolbachia*'s navigation through the developing oocyte, we first characterized this trait in 8 *Wolbachia* strains in their respective hosts: *w*Pan in *D. pandora*, *w*Nik in *D. nikananu*, *w*Cha in *D. chauvacae*, *w*Ha in *D. simulans*, *w*Tsa in D. *tsacasi*, *w*Boc in *D. bocki*, *w*Ana in *D. ananassae*, and *w*Mel in *D. melanogaster*. All 8 strains exhibited a distinct anterior localization during mid-oogenesis (Fig. 2). It is interesting that this localization occurs during stage 5 of oogenesis, which, in *D. melanogaster*, is prior to the localization of all known anterior axis determinants. Thus, *Wolbachia* likely relies on as yet undiscovered anteriorly concentrated factor(s).

Wolbachia exhibits 3 distinct distributions with respect to posterior localization in the mature *Drosophila* oocyte

Concomitant with microtubule rearrangement during stages 7 and 8, *w*Mel *Wolbachia* are released from the oocyte anterior resulting in the dispersal of the bacteria throughout the entire length of the oocyte with a fraction concentrating at the posterior pole (Ferree *et al.* 2005). The posterior dispersal of *Wolbachia* requires the plus-end motor protein kinesin (Serbus and Sullivan 2007). Maintenance of those *Wolbachia* that reach the posterior pole relies on a stable association with key pole plasm components (Serbus *et al.* 2011).

We next examined the oocytes of 18 *Drosophila* species infected with 19 diverse *Wolbachia* strains ($N = 72$ total oocytes) to test the hypothesis that oocyte posterior distributions vary. Unlike the conserved anterior localization, *Wolbachia* exhibit 3 distinct patterns of posterior localization in stage 10 oocytes. As shown in Fig. 3 and Supplementary Fig. 5a, 8 *Wolbachia* strains exhibit a localization pattern similar to that observed for *w*Mel in *D. melanogaster* with the bulk of *Wolbachia* evenly distributed throughout the oocyte, and a large fraction concentrated at the posterior pole. We refer to this pattern as *posteriorly localized*.

Our analysis revealed 4 *Wolbachia* strains manifested a 2nd pattern in which the vast majority of *Wolbachia* localized to a distinct cluster at the posterior pole and only few *Wolbachia* are distributed throughout the remainder of the oocyte (Fig. 3 and Supplementary Fig. 5b). In contrast to the pattern described above, rather than being distributed in a wide arc along the posterior pole, they are tightly centered at the extreme posterior region of the oocyte (Fig. 3b). We refer to this pattern as *posteriorly clumped*.

Finally, 7 *Wolbachia* strains exhibit a 3rd pattern in which *Wolbachia* are distributed throughout the entire oocyte but there are few to no bacteria concentration at the posterior pole (Fig. 3

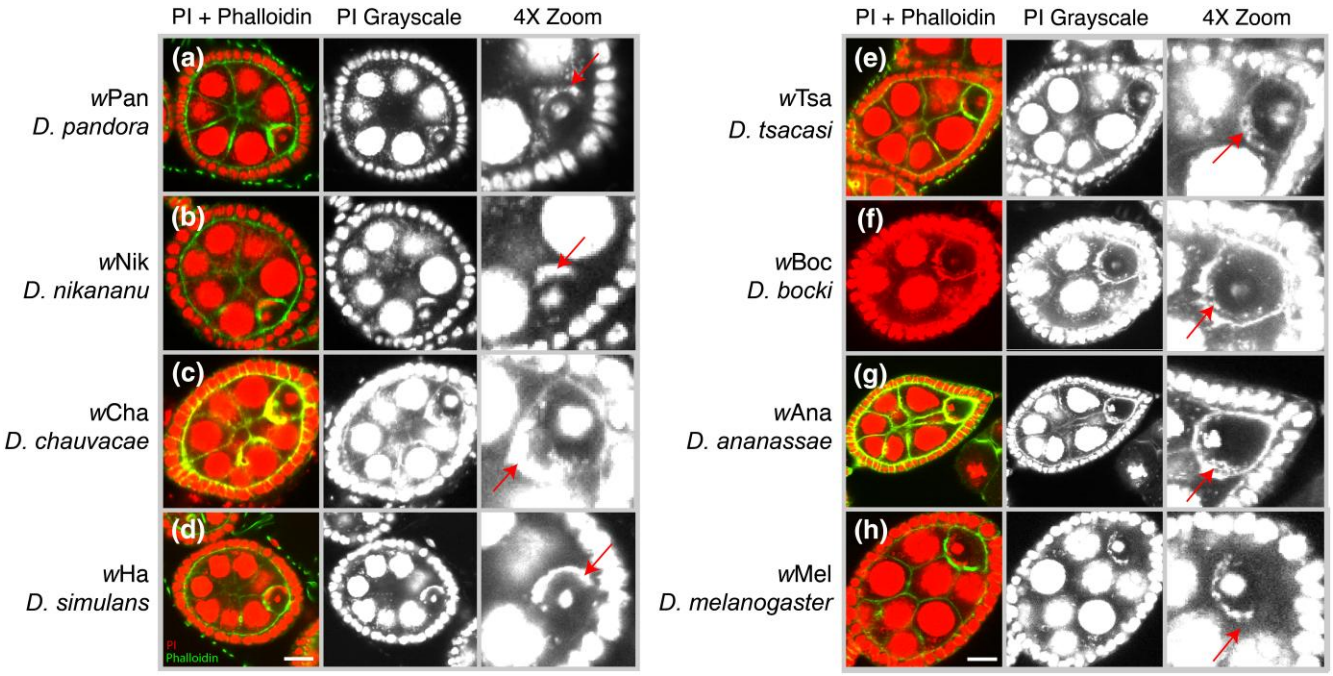

Fig. 2. Conserved *Wolbachia* anterior localization during early oogenesis (stages 4 and 5). *Wolbachia* and host DNA stained with PI (red) and actin with phalloidin (green) shown in the left most column. Grayscale of PI channel shown in the middle. Four times zoom-in around the oocyte shown on the right. All of the 8 *Wolbachia* strains examined concentrate at the anterior cortex of the oocyte at this stage. Red arrows highlight *Wolbachia*'s anterior localization positioning for a) *w*Pan in *D. pandora*, b) *w*Nik in *D. nikananu*, c) *w*Cha in *D. chauvacae*, d) *w*Ha in *D. simulans*, e) *w*Tsa in *D. tsacasi*, f) *w*Boc in *D. bocki*, g) *w*Ana in *D. ananassae*, and h) *w*Mel in *D. melanogaster*. Oocytes are approximately 50–75 μM in size.

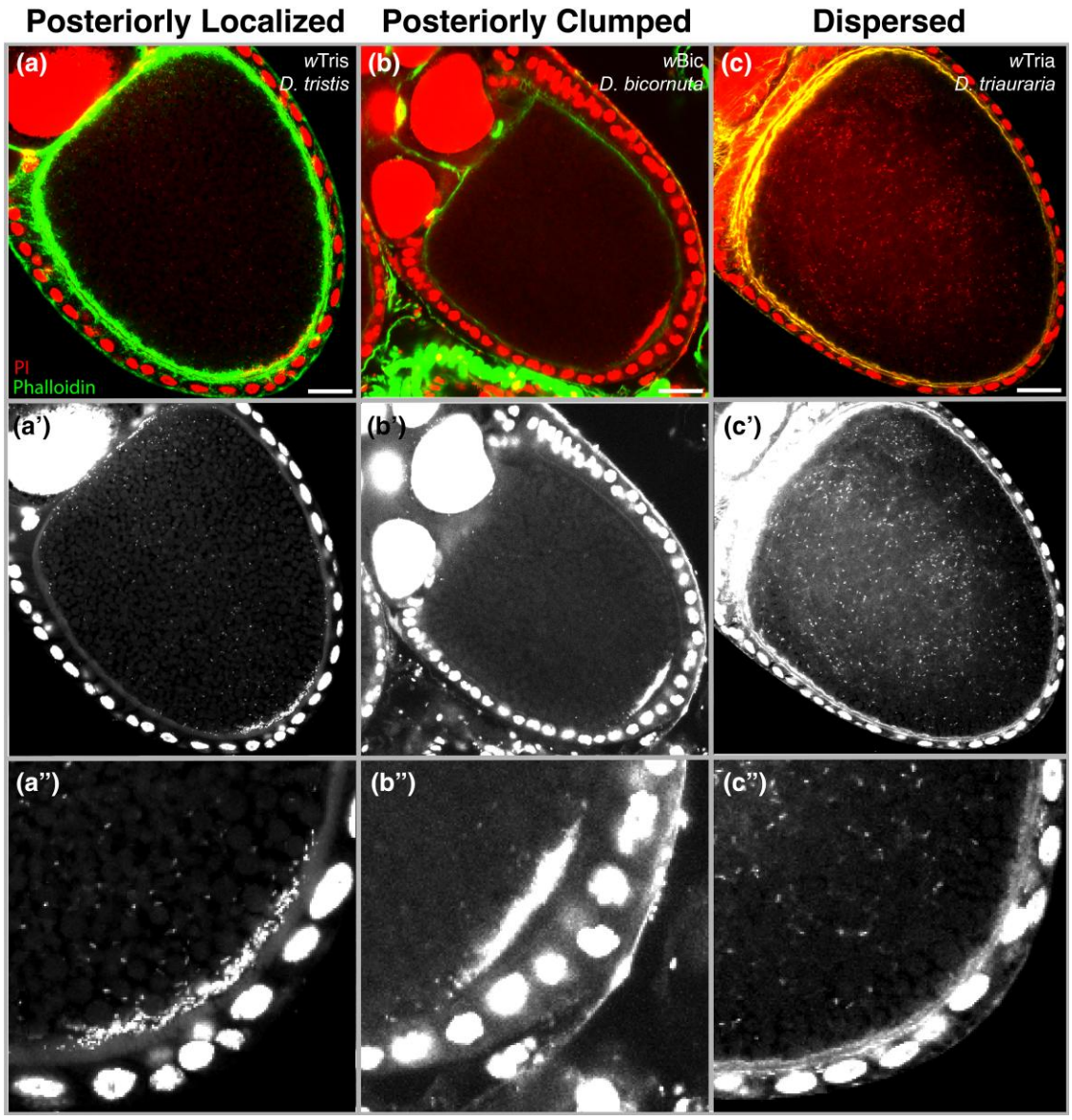

Fig. 3. Three distinct patterns of posterior *Wolbachia* localization during late-stage oogenesis. Confocal micrographs of *Drosophila* oocytes DNA-stained with PI (red) and actin-stained with phalloidin (green) show representative examples of a) posteriorly localized *w*Tris in *D. tristis*, b) posteriorly clumped *w*Bic in *D. bicornuta*, and c) dispersed localization of *w*Tria in *D. triauraria*. Second row depicts single-channel images of PI staining. Third row depicts an enlarged PI-stained image of the posterior region of each oocyte. Scale bars set at 25 μM.

and Supplementary Fig. 5c). The lack of the *Wolbachia* at the posterior pole was unexpected as this was thought to be necessary for incorporation into the germline of the next generation. We refer to this pattern as *dispersed*.

Quantification of *Wolbachia* oocyte distribution patterns

We used one-way ANOVAs to test whether the 3 classes (posteriorly localized, posteriorly clumped, and dispersed) differ statistically in quantitative estimates of *Wolbachia* abundance in the whole oocyte, at the posterior region, and at the posterior cortex (Supplementary Fig. 6). We defined the posterior region as the posterior 12.5% of the oocyte and the posterior cortex as the narrow cortical region of Vasa expression (Russell *et al.* 2018), and we then measured total *Wolbachia* abundance in each region as the corrected total cell fluorescence (CTCF). We found that *Wolbachia* abundance differs significantly among the 3 classes ($F_{(2,69)} = 6.2$, $P = 0.003$), with Tukey's multiple comparisons indicating that the clumped class has significantly more *Wolbachia* in whole oocytes than the localized group ($P = 0.002$). The 3 classes also differed significantly in the amount of *Wolbachia* in the posterior region ($F_{(2,69)} = 23.09$, $P < 0.001$), such that the dispersed class has significantly fewer *Wolbachia* at the posterior than the clumped ($P < 0.001$) and localized ($P < 0.001$) groups. Finally, the 3 classes also differ in the amount of *Wolbachia* at the posterior cortex ($F_{(2,64)} = 38.12$, $P < 0.001$). Here, multiple comparisons indicate that all 3 classes significantly differ in levels of *Wolbachia* at the posterior cortex: the clumped class has the most *Wolbachia*, followed by localized, and then dispersed (Supplementary Fig. 6). Mean estimates of *Wolbachia* abundance (CTCF) for each *Wolbachia* strain and host species are shown in Table 1.

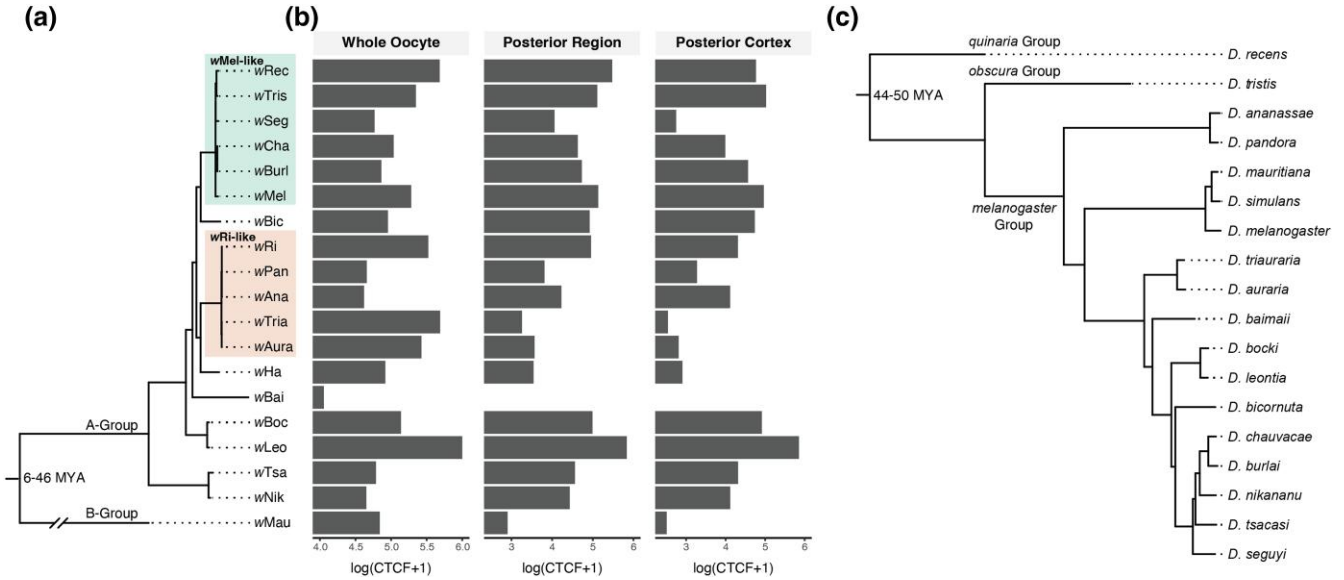

Fig. 4. *Wolbachia* abundance in the posterior region of host oocytes exhibits phylogenetic signal on the *Wolbachia* phylogeny. a) Estimated Bayesian phylogram for the 19 A- and B-group *Wolbachia* strains included in tests for phylogenetic signal. b) Mean estimates of *Wolbachia* abundance (log-transformed CTCF) in the whole oocyte, posterior region, and the posterior cortex. *Wolbachia* abundance in the posterior region has significant phylogenetic signal [$\lambda = 0.982$ (0, 0.998), $P = 0.021$], suggesting *Wolbachia*-associated factors determine *Wolbachia* abundance in the oocyte posterior. c) Estimated Bayesian phylogram of *Drosophila* host species using 20 conserved single-copy genes. *Wolbachia* and host divergence times in millions of years (MYA) are reproduced from Meany *et al.* (2019) and Suvorov *et al.* (2022), respectively. The *Wolbachia* and host trees are generally discordant (see Supplementary Fig. 4), as expected with frequent horizontal *Wolbachia* acquisition (Turelli *et al.* 2018).

Wolbachia abundance in the oocyte posterior has strong phylogenetic signal

We hypothesized that the diversity of *Wolbachia* localization patterns may be due to *Wolbachia*-associated factors, implying that closely related *Wolbachia* strains would exhibit similar localization patterns in host oocytes. We used the phylogram describing the evolutionary relationships among *Wolbachia* strains to test whether patterns of *Wolbachia* localization exhibit a phylogenetic signal using Pagel's λ (Pagel 1999; Hague *et al.* 2020b, 2021) (Fig. 4). A λ value of 1 would be consistent with trait evolution that entirely agrees with the *Wolbachia* phylogeny (i.e. strong phylogenetic signal supporting a role of *Wolbachia* factors), whereas a value of 0 would indicate that trait evolution occurs independently of phylogenetic relationships (Pagel 1999; Freckleton *et al.* 2002). Most notably, we found that *Wolbachia* abundance (CTCF) in the posterior region exhibits a strong, significant phylogenetic signal [$\lambda = 0.982$ (0, 0.998), $P = 0.021$]. *Wolbachia* abundance at the posterior cortex also has a high, but non-significant λ value [$\lambda = 0.959$ (0, 0.995), $P = 0.683$]. Here, the large confidence intervals and our simulations suggest that a larger *Wolbachia* phylogeny ($N = 25$ and 50 *Wolbachia* strains) is required to detect a significant signal of $\lambda > 0$ (Supplementary Fig. 7). These results highlight differences in patterns of *Wolbachia* localization between the *w*Mel- and *w*Ri-like *Wolbachia* clades (Fig. 3). Closely related *w*Mel-like *Wolbachia* tend to occur at a higher abundance in the posterior region of oocytes, whereas the *w*Ri-like strains are generally more dispersed. We found no evidence that *Wolbachia* abundance in the whole oocyte exhibits a phylogenetic signal [$\lambda < 0.001$ (0, 0.753), $P = 1$].

The correlation between *Wolbachia* localization in oocytes and phylogenetic divergence implies that factors in the *Wolbachia* genome determine *Wolbachia* abundance at the oocyte posterior. Because these distributions likely involve direct interactions between *Wolbachia* and the host cytoplasm, we focused on 6 major *Wolbachia* surface proteins: the 3 *wsp* paralogs (WD_1063/*wsp*, WD_0009/*wspB*, and WD_0489/*wspC*), as well as WD_0501, WD_1041, and WD_1085 (Supplementary Table 3). We tested whether sequence divergence at any of these candidate loci predicts *Wolbachia* localization patterns. Specifically, we tested whether gene trees of the *Wolbachia* surface proteins (Supplementary Fig. 8) exhibit a phylogenetic signal, using the methods described above. One surface protein (WD_1085) stood out with especially strong evidence of a phylogenetic signal, with significant departures from $\lambda = 0$ for *Wolbachia* abundance at the posterior region [$\lambda = 0.974$ (0, 0.998), $P = 0.001$] and the posterior cortex [$\lambda = 0.942$ (0, 0.994), $P = 0.028$]. In addition, *Wolbachia* abundance at the posterior region also exhibited significant phylogenetic signal on the gene tree of WD_0501 [$\lambda = 0.992$ (0.521, 1), $P = 0.022$]. All tests for phylogenetic signal using *Wolbachia* gene trees are summarized in Supplementary Table 4.

Motivated by previous successful analysis of *Wolbachia* protein function through ectopic expression in yeast, we expressed codon-optimized forms of WD_1085 and WD_0501 in yeast using a galactose-inducible promoter (Sheehan *et al.* 2016; Rice *et al.* 2017). Under normal growth conditions, ectopic expression of both genes inhibited growth, with WD_1085 exhibiting a more pronounced inhibition (Supplementary Fig. 9). Because *Wolbachia* exhibits a close association with microtubules, we also assayed whether ectopic expression of these genes enhanced the growth defects in situations in which the microtubule spindle assembly checkpoint was compromised by a mad1 mutation (Luo *et al.* 2018), or when the microtubules were compromised directly through the addition of benomyl. As indicated in Supplementary Fig. 9, ectopic expression of WD_1085 significantly inhibited growth when both the microtubules and spindle checkpoint were compromised. These results suggest that ectopic WD_1085 expression perturbs microtubule function.

We recently found that the surface protein WD_0009 (*wspB*) is pseudogenized due to a premature stop codon in a tropical *w*Mel

variant sampled from Australia, which seems to influence *w*Mel abundance in stage 10 oocytes when hosts are reared in the cold (Hague *et al.* 2022). Here, we did not find that the *wspB* gene tree exhibits phylogenetic signal related to *Wolbachia* oocyte abundance (Supplementary Table 4); however, we note that *wspB* appears to be pseudogenized in a number of other *Wolbachia* strains in addition to tropical *w*Mel. We found derived deletions of varying length in the *wspB* sequences of *w*Ha and *w*Bai beginning at nucleotide position 256, both of which produce frame shifts that generate multiple downstream stop codons (Supplementary Fig. 10). In addition, *w*Boc and *w*Leo share a large insertion starting at bp position 351. Because the insertions contain a contig break, we were unable to resolve the full length of the insertion. Lastly, *w*Bic contains a 104-bp insertion at bp position 647 that creates multiple downstream stop codons. These results suggest that the surface protein *wspB* has become pseudogenized at least 4 times in different *Wolbachia* lineages. Notably, the *Wolbachia* strains with a putatively pseudogenized version of *wspB* do not differ from the other strains in mean *Wolbachia* abundance in whole oocytes (Wilcoxon rank sum test, $W = 36$, $P = 0.964$), the posterior region ($W = 37$, $P = 0.893$), or the posterior cortex ($W = 41$, $P = 0.622$). This suggests that pseudogenization of *wspB* does not influence the diverse patterns of *Wolbachia* localization observed here. To gain insight into *wspB* cellular function, we ectopically expressed this gene (and the other *wsp* paralogs: WD_1063/*wsp* and WD_0489/*wspC*) in yeast using the galactose expression system described above. Using this system, we found that ectopic expression of codon-optimized *wspB* and *wsp* significantly inhibited yeast growth (Supplementary Fig. 11). Ectopic expression of *wspC* kills the cells. Based on similar ectopic expression studies (Sheehan *et al.* 2016), the suppression is likely due to *Wolbachia* proteins interacting with and disrupting the function of yeast components and cellular processes that are conserved and performing similar functions in insect cells.

Lastly, we ran similar phylogenetic analyses using the host phylogeny (as opposed to *Wolbachia*) to test whether host-associated factors might also contribute to the diverse *Wolbachia* distribution patterns in fly oocytes (Supplementary Fig. 1). We generally found that *Wolbachia* localization patterns do not exhibit a phylogenetic signal on the host tree. *Wolbachia* abundance in whole oocytes [$\lambda = 0.365$ (0, 0.856), $P = 0.656$], at the posterior region [$\lambda < 0.001$ (0, 0.658), $P = 1$], and at the posterior cortex [$\lambda < 0.001$ (0, 0.637), $P = 1$] did not exhibit phylogenetic signal using the host phylogram, implying that host-associated factors are not as important in determining diverse *Wolbachia* localization patterns in oocytes.

Vertical transmission in some host species likely relies on *Wolbachia* entering the germline from neighboring somatic tissues

Because *Wolbachia* strains with a dispersed localization do not localize to the pole, one would expect maternal transmission to be compromised. However, previous studies demonstrate that some of these *Wolbachia*, such as the B-group strain *w*Mau in *D. mauritiana*, have high maternal transmission rates under standard laboratory conditions (i.e. constant 25°C), equivalent to that of *w*Mel in *D. melanogaster* (Meany *et al.* 2019; Hague *et al.* 2022). These findings suggest that, in addition to strict germline-to-germline transmission, *Wolbachia* may utilize alternative routes of maternal transmission. Because numerous vertically inherited endosymbionts are transmitted via cell-to-cell transmission from the soma to the germline (Frydman *et al.* 2006; Russell *et al.* 2019), we explored whether *Wolbachia* that infect *Drosophila* exploits this strategy.

To determine the developmental stage during which somatic *Wolbachia* might invade the germline in dispersed species, we focused on B-group *w*Mau in *D. mauritiana*. Initially, we examined the female germline (oocytes) of the 3rd instar larva for the presence of *Wolbachia*. For comparison, we also examined the oocytes of *w*Mel-infected *D. melanogaster* (a strain with a posteriorly localized concentration of *Wolbachia*) 3rd instar larvae using anti-FtsZ to mark the *Wolbachia* and anti-Vasa to mark the germline. As shown in Fig. 5, *Wolbachia* are abundantly present in ring-like patterns in many of the Vasa-positive cells in the center of the developing oocyte. Imaging the oocytes of *w*Mau-infected *D. mauritiana* revealed a similar pattern with *Wolbachia* concentrated in the developing female germline of the 3rd instar larva (Fig. 5). Images of *w*Ri in *D. simulans* as well as *w*Bic in *D. bicornuta*—strains with a dispersed localization and posteriorly clumped localization in mature oocytes, respectively—displayed the same ring-like structure in the developing oocyte of the 3rd instar larva, although they appeared to have a much higher titer than *w*Mau or *w*Mel (Fig. 5). This indicates that in these species, in which vertical transmission occurs with a few or no *Wolbachia* present at the posterior site of germline formation in mature adult oocytes, *Wolbachia* are able to occupy the germline at some point between the final stages of oocyte maturation and development of the fertilized egg into a 3rd instar larva. Presumably, the source of the *Wolbachia* is via invasion from neighboring somatic cells.

To determine if *Wolbachia* occupied the germline prior to the 3rd instar larval stage, we examined the newly formed germline of late blastoderm and cellularized embryos. At this stage, newly formed germline cells, known as the pole cells, form a distinct cluster of cells at the extreme posterior to the embryo. In all the 4 strains described above, using PI or anti-*Wolbachia* staining, *Wolbachia* are readily found in these posterior germline cells (Fig. 6). Imaging *w*Mau in *D. mauritiana* early blastoderm embryos revealed the presence of *Wolbachia* in the posterior pole cells. This observation narrows the time window in which *Wolbachia* invades and occupies the germline from between the final stages of oocyte maturation to early blastoderm formation. Images taken of *D. mauritiana* in 1-h-old embryos also showed *w*Mau positioned in the posterior pole, narrowing the developmental window of *Wolbachia* germline occupation between the final stages of oocyte maturation to 1 h after fertilization (Fig. 6). Interestingly, Veneti *et al.* (2004) reported that *w*Mau exhibits an anterior localization pattern during *D. mauritiana* embryogenesis; however, we found no such pattern for any of the embryos examined.

Our findings motivated us to examine *w*Mau in *D. mauritiana* oocytes just prior to egg deposition. Previous studies found that in many infected *Drosophila* species, *Wolbachia* is concentrated in the most posterior positioned follicle cells (Kamath *et al.* 2018). These somatically derived cells, known as polar cells, directly contact the oocyte posterior pole plasm. In accord with Kamath *et al.* (2018), we find that *Wolbachia* are sporadically distributed in subsets of more anterior positioned follicle cells encompassing the oocyte. *w*Mau presence in the polar follicle cells is a consistent feature in every *D. mauritiana* oocyte examined (Fig. 7). Given their position, these *w*Mau-infected cells are likely the polar follicle cells. These observations raise the possibility that *Wolbachia* in the polar follicle cells may be a somatic source of germline *w*Mau in *D. mauritiana*. In spite of much effort, however, we have not been able to find cytological evidence for this hypothesis.

To determine the extent to which *Wolbachia* polar follicle cell localization is conserved, we analyzed *Wolbachia* localization in

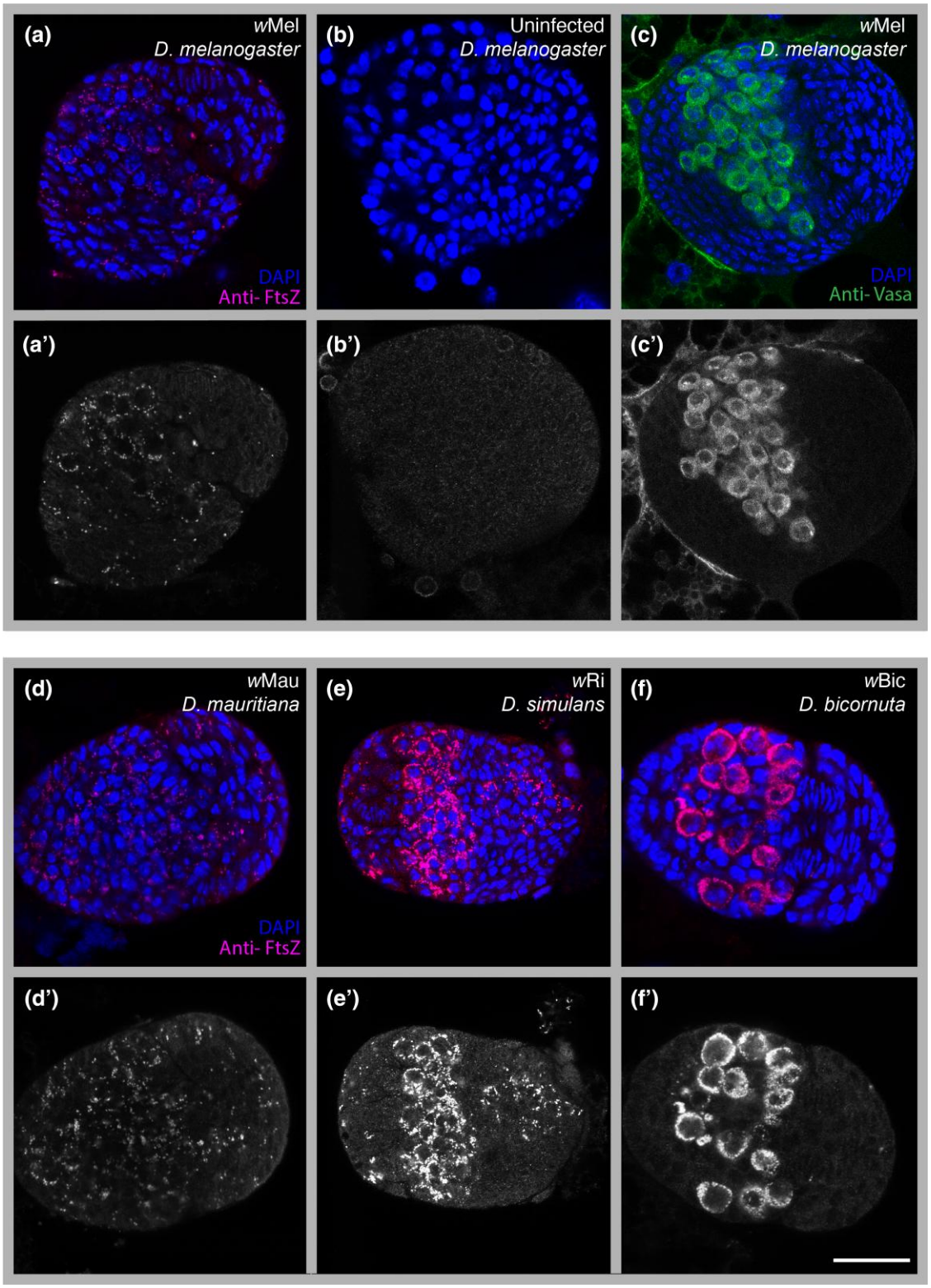

Fig. 5. *Wolbachia*'s presence around the 3rd instar larval germline, in multiple *Drosophila* hosts. *w*Mel *Wolbachia* stained with anti-FtsZ can be seen for *D. melanogaster*, in a) shown in pink. Cells are marked with DAPI (blue). a') Grayscale channel of anti-FtsZ staining. b) Uninfected ovary for *D. melanogaster* and b') grayscale channel for uninfected antibody binding. Germline location marked with anti-Vasa shown in green c) and grayscale channel c'). *w*Mau *Wolbachia* localization in the ovary for *D. mauritiana* shown in d) and grayscale channel d'). *w*Ri and *D. simulans* shown in e) and grayscale e'). f) *w*Bic and *D. bicornuta* and f') grayscale channel. Scale bar shown at 25 μM.

the polar and more anterior follicle cells for 7 *Wolbachia* strains with the following patterns: dispersed ($N = 3$), posteriorly localized ($N = 3$), and posteriorly clumped ($N = 1$) (Fig. 7). We scored for the presence of follicle cell *Wolbachia* in each oocyte ($N = 75$) using the following criteria: the presence of *Wolbachia* in either both or 1 of the posterior polar follicle cells (Fig. 7d) and the presence of

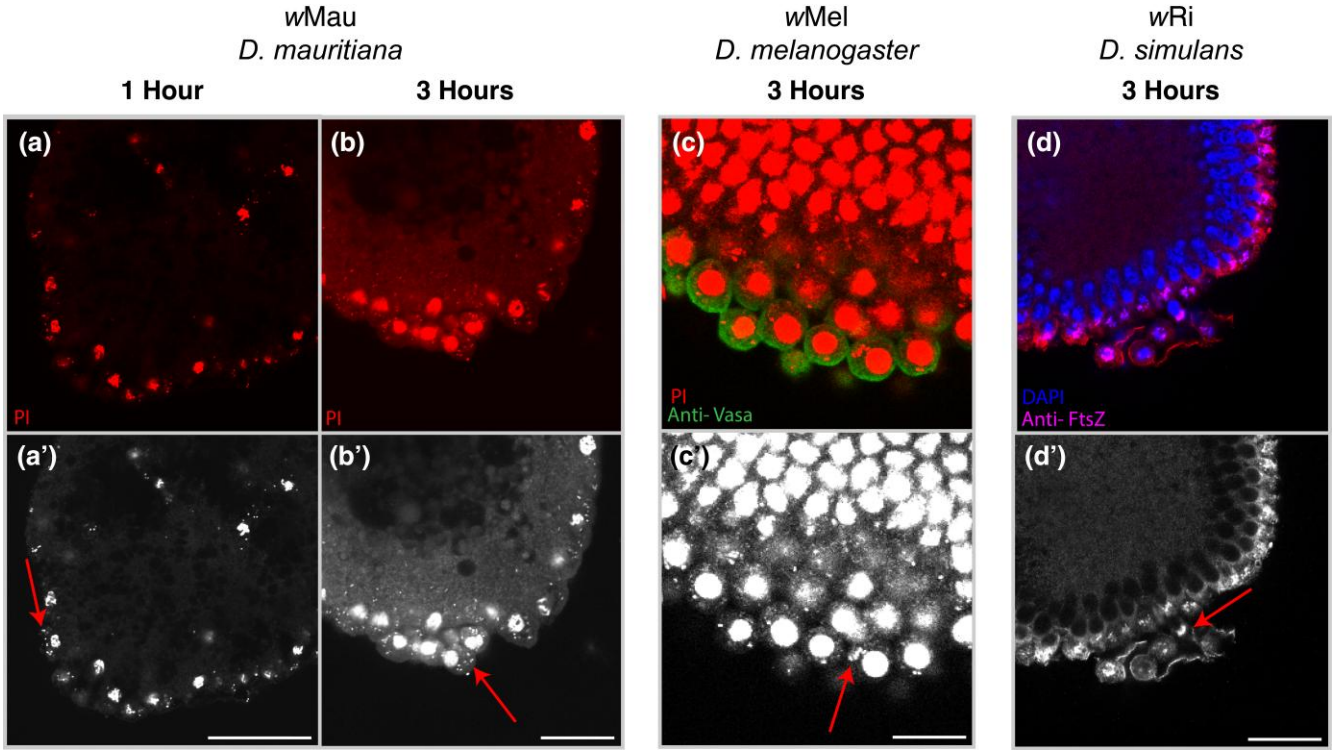

Fig. 6. *Wolbachia*'s presence in the newly formed germline cells of late blastoderm and cellularized embryos. a) One hour *D. mauritiana* (*w*Mau) embryo stained with PI. a') Grayscale of PI channel. b) Staining of 2–3 h developed *D. mauritiana* (*w*Mau) embryo with PI. b') Grayscale of PI channel. c) PI and anti-Vasa (green) staining of *w*Mel *Wolbachia* in 2–3 h *D. melanogaster* embryo. c') Grayscale of PI channel. d) Anti-FtsZ/DAPI staining for *w*Ri *Wolbachia* in *D. simulans*. d') Grayscale of anti-FtsZ channel. Scale bars set at 25 μM.

Wolbachia in the more anteriorly localized follicle cells (Fig. 7e). This analysis revealed that in a high percentage of oocytes from dispersed strains (a lack of the *Wolbachia* at the oocyte posterior), *Wolbachia* are frequently present in the posterior polar follicle cells. In contrast, with the exception of wMel, oocytes examined from strains in which *Wolbachia* are posteriorly concentrated (the posteriorly localized and clumped strains), few possess *Wolbachia* in the posterior follicle cells. The 7 *Wolbachia* strains exhibit significant variation in whether *Wolbachia* cells are found in the polar follicle cells ($\chi^2_{(12)} = 65.15$, $P < 0.001$) (Fig. 7d). In particular, the divergent B-group strain *w*Mau stood out with a large proportion of oocytes containing *Wolbachia* in the 2 polar follicle cells. The A-group *w*Mel strain also had a large portion of oocytes with *Wolbachia* in 1 or 2 of the polar cells. We also found that the *Wolbachia* strains differ in whether *Wolbachia* cells are found in the other more anterior follicle cells ($\chi^2_{(6)} = 43.29$, $P < 0.001$) (Fig. 7e). Again, the *w*Mau and *w*Mel strains had a large portion of oocytes with *Wolbachia* in the other more anterior follicle cells encompassing the oocyte. Of note, for *w*Mau in *D. mauritiana*, every oocyte had at least 1 of their polar cells filled with *Wolbachia*, observationally at a higher titer (Fig. 7). This suggests that in the dispersed strains, vertical transmission may be achieved via invasion of *Wolbachia* from the polar follicle cells, particularly for the divergent B-group *w*Mau strain.

Discussion

Vertical transmission through the female lineage is a common strategy for many endosymbionts. These endosymbionts achieve high efficiencies of maternal transmission either through direct germline-to-germline transmission or invasion of the maternal germline through neighboring somatic cells (Russell *et al.* 2019). Because the former involves a continuous presence in the germline while the latter requires navigating a soma-to-germline passage, it is expected that each requires distinct interactions with and manipulations of host cellular processes. Thus, it would be expected that a given endosymbiont would have evolved to utilize 1, but not both of these strategies. Here, we explore this issue by examining cellular aspects of *Wolbachia* vertical transmission. In contrast to expectations, our comprehensive analysis demonstrates that *Wolbachia* likely rely on both strict germline-to-germline and soma-to-germline vertical transmission strategies. Which strategy employed varies among *Wolbachia* strains.

The initial anterior *Wolbachia* localization in the developing oocyte appears to be a conserved aspect of *Wolbachia* transmission, as all 8 strains examined exhibit this localization. It is striking that this localization occurs prior to any known anterior determinant, indicating *Wolbachia* may associate with an as yet undiscovered host factor concentrated at the anterior. That this localization is conserved suggests that it has a functionally significant, but currently unknown role in *Wolbachia* transmission. While anteriorly localized, the amount of *Wolbachia* dramatically increases. Whether *Wolbachia* replication, transport from the nurse cells, or both are responsible for this increase is unknown. The anterior location may be a rich source of membrane for *Wolbachia* replication. The anterior localization also results in a high concentration of *Wolbachia* that closely associate with, and perhaps influences, the status of the oocyte nucleus.

To our surprise, we discovered that immediately after the release of *w*Mel *Wolbachia* from its anterior position in the oocyte (stage 6), the amount of *Wolbachia* in the oocyte dramatically decreases (see Fig. 1, stage 6 and Supplementary Fig. 3). This

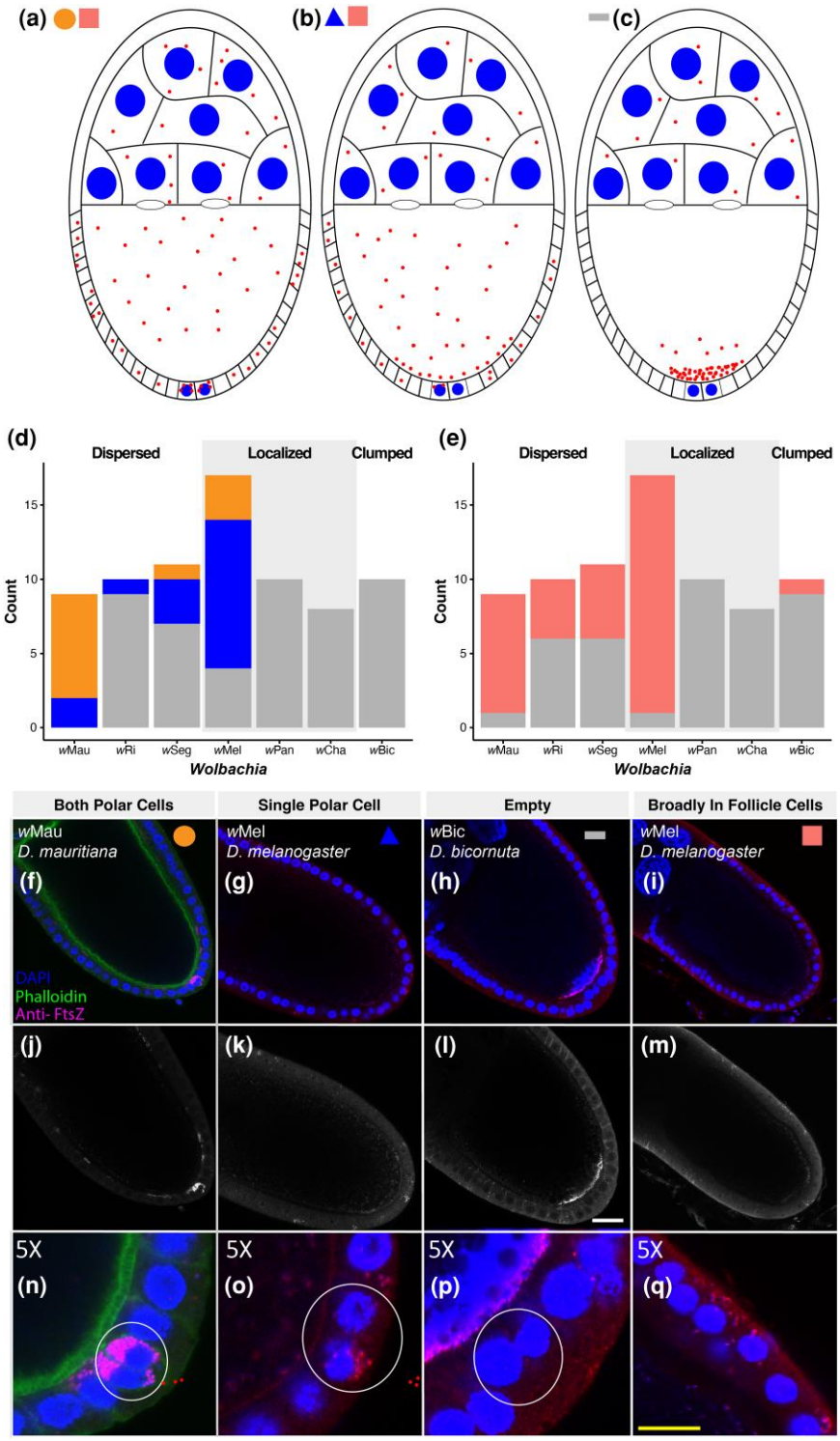

Fig. 7. The A-group *w*Mel and B-group *w*Mau *Wolbachia* strains are frequently found in the polar follicle cells, as well as other follicle cells. a)–c) Schematic of categories used for description of follicle cell *Wolbachia*. a) Dispersed localization pattern shown, both polar cells infected, with *Wolbachia* broadly present in follicle cells. b) Posteriorly localized pattern shown, 1 polar cell infected, with *Wolbachia* broadly present in follicle cells. c) Posteriorly clumped pattern shown, with no *Wolbachia* present in the polar cells or other follicle cells. d) *Wolbachia* quantification in the polar follicle cells during oogenesis stages 9 and 10. *Wolbachia* were quantified in midsections of each oocyte that displays unique posterior localization patterns: dispersed, posteriorly localized, and posteriorly clumped. For each strain, the count is shown for the number of oocytes observed with *Wolbachia* present in both polar follicle cells (orange), only 1 polar cell (blue), and neither polar cell (gray). e) Counts of oocytes observed with *Wolbachia* present anywhere in the follicle cells (pink) or with *Wolbachia* absent (gray). f) Representative anti-FtsZ staining of *w*Mau in *D. mauritiana* (dispersed class) present in both polar follicle cells (corresponding to orange labels above). g) Representative staining of *w*Mel in *D. melanogaster* (posteriorly localized class) present in only 1 polar cell (blue labels above). h) Representative staining of *w*Bic in *D. bicornuta* (posteriorly clumped class) absent in both polar cells (gray labels above). i) Representative staining of *w*Mel in *D. melanogaster* (posteriorly localized class) broadly present in anterior follicle cells (pink labeling above). j)–m) Grayscale anti-FtsZ channel of respective composite images above. n)–q) Five times zoom of polar cells, with circles highlighting representative staining in the area. Scale bar set at 25 μM.

suggests that the *Wolbachia* are transported back into the nurse cell complex. The functional significance of this clearing of *Wolbachia* from the oocyte is unknown. The retreat of *Wolbachia* occurs during the time when the anteriorly positioned oocyte nucleus and neighboring follicle cells signal one another in order to establish the dorsal ventral axis (Merkle *et al.* 2020). Perhaps, *Wolbachia* exits the oocyte in order to not disrupt this process. Given the orientation of microtubules at this stage, it is likely *Wolbachia* rapidly exits the oocyte through an association with the plus-end–directed motor protein kinesin.

Following microtubule reorientation and the return of *Wolbachia* to the oocyte, *Wolbachia* spreads posteriorly throughout the entire oocyte relying on the host motor protein kinesin (Serbus and Sullivan 2007). All of the *Wolbachia* strains examined are distributed toward the posterior regions suggesting the interaction with kinesin is also conserved. How *Wolbachia* engages these motor proteins is unknown. Surprisingly, none of the known host kinesin linker proteins are utilized by *Wolbachia*, suggesting *Wolbachia* may interact directly with kinesin (Russell *et al.* 2018).

It is after this stage, in which *Wolbachia* is distributed throughout the oocyte, that we observe variability among the *Wolbachia* strains, with each falling into 1 of 3 distinct classes: 2 distinct classes in which *Wolbachia* concentrate at the posterior (posteriorly localized and posteriorly clumped) and 1 class in which *Wolbachia* fail to exhibit a posterior concentration (dispersed). The former 2 classes are distinguished by whether the vast majority (posteriorly clumped) or only a small fraction of the *Wolbachia* localize to the posterior pole (posteriorly localized). Here, our phylogenomic analyses revealed a strong correlation between *Wolbachia* posterior abundance and *Wolbachia* phylogenetic relationships. Generally, we find that closely related *w*Mel-like *Wolbachia* occur at higher abundance at the oocyte posterior, whereas *w*Ri-like *Wolbachia* exhibit a more dispersed distribution (Fig. 4). These results suggest that factors intrinsic to *Wolbachia* help determine posterior localization patterns, which is consistent with previous *Wolbachia* transplantation studies demonstrating that posterior localization is determined by *Wolbachia* rather than host factors (Poinsot *et al.* 1998; Veneti *et al.* 2004; Serbus and Sullivan 2007). Below, we discuss how specific factors might contribute to variation in *Wolbachia* localization patterns.

The posteriorly localized class, in which only a small fraction localize to the posterior pole, can be explained by previous work demonstrating that *w*Mel is a weak competitor for kinesin; both *Wolbachia* and germplasm components rely on kinesin for transport to the posterior pole (Russell *et al.* 2018). It is thought that *Wolbachia* has evolved to be a weak competitor because interference with the transport of essential germplasm components and thus germplasm formation may be disadvantageous for *Wolbachia* proliferation. The other posterior class (posteriorly clumped) is strikingly similar to that observed for *w*Mel in *D. melanogaster* in which the plus-end motor protein kinesin is overexpressed and excess amounts of *Wolbachia* are transported to the posterior pole (Russell *et al.* 2018). It may be that the posteriorly clumped strains are much better competitors for host kinesin. Alternatively, these strains could occur in host species with naturally much higher levels of host kinesin, although our phylogenetic analysis did not support a role of host factors. Functional work will be required to formally test these hypotheses. In particular, it would be interesting to investigate whether there are instances in which *Wolbachia* disrupts the anterior–posterior (A-P) axis because of its accumulation at the posterior pole.

The posterior pole concentration among *Wolbachia* strains may also differ due to variability in the ability of *Wolbachia* to stably associate with the pole plasm. Previous studies demonstrated that *Wolbachia* posterior pole concentration requires intact pole plasm (Serbus and Sullivan 2007). For example, in *oskar* mutations, a key pole plasm determinant, *w*Mel *Wolbachia* fails to accumulate at the posterior region (Hadfield and Axton 1999; Serbus and Sullivan 2007). As described, the oocyte experiences tremendous cytoplasmic streaming requiring posterior components to be anchored directly or indirectly to the cortex (Quinlan 2016). This variability could be due to differences in the ability of *Wolbachia* to compete with other pole plasm components such as mitochondria for binding sites. Alternatively, the host species may vary in the extent to which their pole plasm accommodates *Wolbachia*. These alternatives can be explored through trans-infection studies.

It is likely that the composition of *Wolbachia* surface proteins play a major role in the extent of posterior localization. Our phylogenetic analyses revealed that the gene trees of 2 candidate surface proteins, particularly WD_1085, are strongly associated with *Wolbachia* localization patterns. The WD_1085 protein has sequence and structural homology to the bacterial outer membrane protein BamA, which consists of a large periplasmic domain attached to a 16-stranded β-barrel domain (Supplementary Fig. 2). BamA is the central subunit of the β-barrel assembly machinery (BAM), which is essential for outer membrane protein biogenesis (Noinaj *et al.* 2013; Doyle and Bernstein 2019). Given this finding, it is intriguing that we find overexpression of BamA is sensitive to disruptions in microtubules, as these cytoskeletal elements are essential for outer membrane biogenesis in mitochondria (Mado *et al.* 2019). It may be that microtubules are also required for *Wolbachia* membrane biogenesis. While we highlight these loci as potential candidates, we note that our results should be interpreted with caution since the WD_1085 gene could be in linkage with other causal loci. Nonetheless, *Wolbachia* surface proteins are generally considered to be strong candidates for interactions with host cells (Werren *et al.* 2008; Baldridge *et al.* 2016; Hague *et al.* 2022).

Interestingly, our phylogenomic analyses did not find a correlation between host phylogenetic relationships and *Wolbachia* localization patterns, suggesting that host-associated factors are less important in determining *Wolbachia* posterior localization. This result contrasts with transplantation studies that indicate hosts may also play a significant role in determining *Wolbachia* abundance (Veneti *et al.* 2004). In addition, genome-wide screens reveal host factors play a major role in determining *Wolbachia* intracellular abundance (White *et al.* 2017b; Grobler *et al.* 2018). Thus, variation in the host proteins that *Wolbachia* engages could still plausibly influence *Wolbachia* localization patterns. This would contrast with other endosymbionts such as *Listeria*, which relies on a surface protein that binds and polymerizes host actin to propel the bacteria within and between host cells (Kühn and Enninga 2020). Because the interaction between ActA and actin is essential for cell-to-cell transmission, natural variants of this interaction and transmission strategy have not been discovered. In addition to *Wolbachia* and host factors, nutrients and other environmental factors have also been shown to influence *Wolbachia* abundance and localization in host oocytes for closely related *w*Mel-like *Wolbachia* strains (Serbus *et al.* 2015; Hague *et al.* 2020a, 2022).

Two classes in which *Wolbachia* concentrates in the posterior pole (posteriorly localized and posteriorly clumped) provide a ready explanation for the cellular mechanisms by which it is vertically transmitted through generations. In every generation, *Wolbachia* targets the site of germline formation in the developing

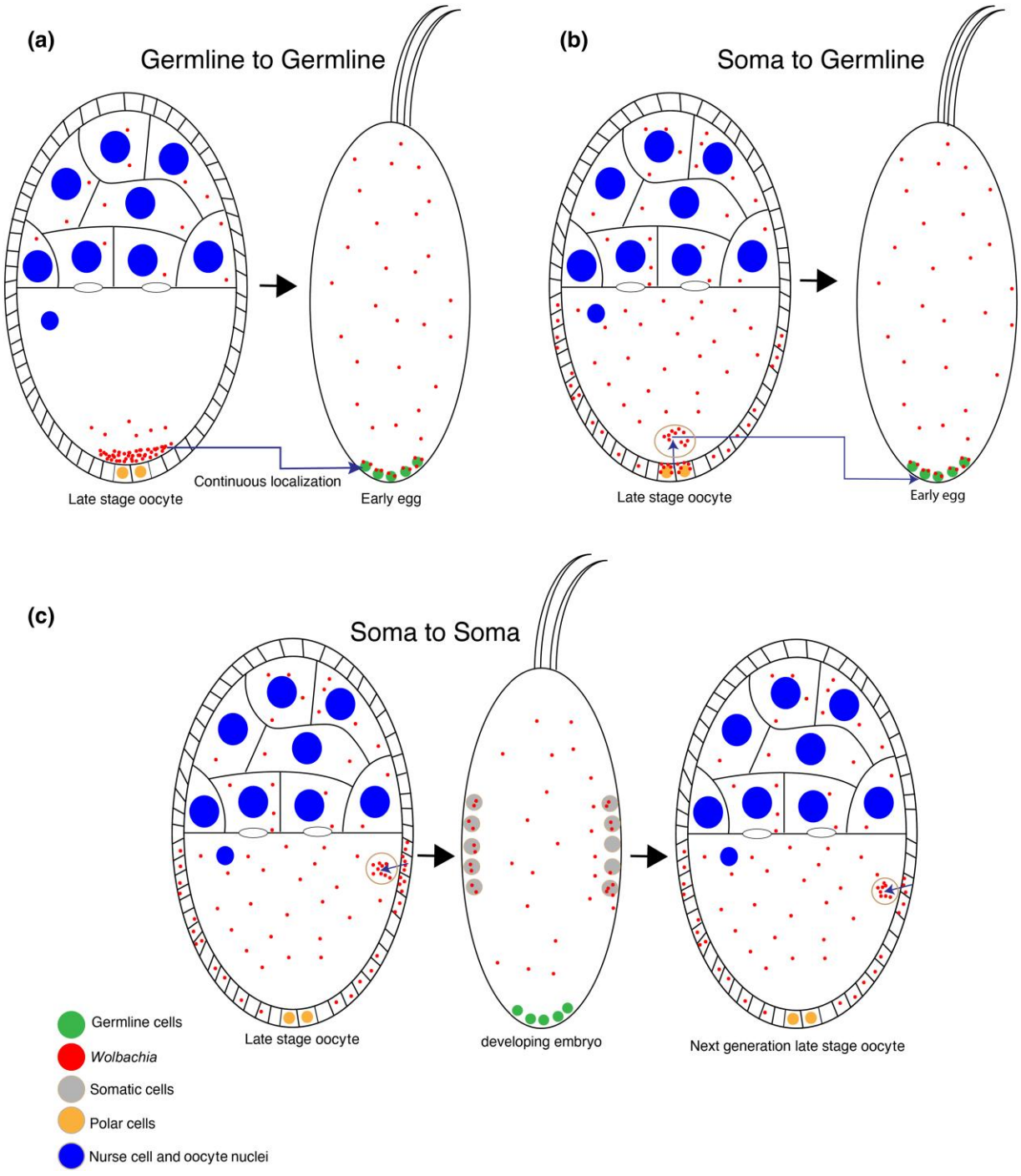

Fig. 8. Multiple routes of *Wolbachia* vertical transmission. a) In *Wolbachia* strains that concentrate at the posterior pole plasm, vertical transmission likely occurs through a continuous maintenance in the germline. b) In strains where no or few *Wolbachia* localize to the posterior pole plasm, vertical transmission likely occurs through *Wolbachia* invading the germline from neighboring somatic cells. c) In theory, vertical transmission could occur through a symbiont invading the oocyte from neighboring somatic cells never associating with the germline.

oocyte. This also explains why strains exhibiting this pattern, such as *w*Mel, exhibit efficient transmission strategies under typical laboratory conditions (Hague *et al.* 2022). The 3rd, distributed class, that exhibits no-to-low *Wolbachia* in the posterior germplasm of the mature oocyte is puzzling. This would be expected to result in embryos lacking *Wolbachia* in the germline. However, within hours after fertilization, *Wolbachia* is clearly present in the germlines of both sexes (Fig. 6). This implies that either these *Wolbachia* strains are capable of invading the germline from neighboring somatic cells or a few undetected *Wolbachia* are delivered late in oogenesis to the posterior pole. Support for the 1st hypothesis comes from the fact that in filarial nematodes, *Wolbachia* germline invasion from the soma has been directly observed (Landmann *et al.* 2012). While germline invasion via cell-to-cell transmission has not been directly observed in insects, a number of lines of evidence indicate that it likely occurs. In *Drosophila* cell culture, *Wolbachia* efficiently undergoes cell-to-cell transmission (White *et al.* 2017a). *Wolbachia* injected into the abdomen of adult

Drosophila females migrate to and occupy the germline and follicle stem cells (Frydman *et al.* 2006). Collections directly from nature reveal some strains with developing oocytes lacking *Wolbachia* (Casper-Lindley *et al.* 2011). In these strains, all of the mature oocytes were infected, suggesting an alternate route of infection via neighboring somatic cells.

As previously hypothesized, given the posterior follicle cells are directly adjacent to the pole plasm, we propose *Wolbachia* present in these follicle cells may be the source of germline *Wolbachia* (Kamath *et al.* 2018). Our results are in accord with and complement previous studies demonstrating *Wolbachia* concentrated in the posterior polar follicle cells in a number of *Wolbachia*-infected species (Kamath *et al.* 2018). For example, in *w*Mau-infected *D. mauritiana*, a dispersed class, there is a striking concentration of *Wolbachia* in the posterior follicle pole cells directly adjacent to the pole plasm. Thus, *Wolbachia* in these somatic cells are well positioned to invade the pole plasm becoming incorporated into the germline of the next generation (Figs. 7 and 8). In contrast, in the posteriorly localized and clumped strains, we found no to few *Wolbachia* in the posterior polar follicle cells. We note that invasion of *Wolbachia* from posterior follicle cells into the germline would require *Wolbachia* to cross the seemingly impenetrable newly formed vitelline membrane, which could suggest alternative sources of germline *Wolbachia*. Nonetheless, taken together, the data strongly argue for a somatic-to-germline route of vertical transmission in some *Drosophila* species.

Among the *Wolbachia* strains examined, *w*Mel stands out as an exception. Not only is it concentrated at the posterior pole of the oocyte, but there is also a large *Wolbachia* concentration in the posterior polar follicle cells. Thus, *w*Mel may maintain both robust germline-to-germline and soma-to-germline modes of transmission. Accordingly, it has a high efficiency of vertical transmission under standard laboratory conditions (but see Hague *et al.* 2022). Notably, we found that *w*Mel and *w*Mau are also both quite prevalent in the more anteriorly located follicle cells of stage 10 oocytes (Fig. 7), raising the possibility that vertical transmission could even occur without *Wolbachia* ever directly associating with the host germline (i.e. soma-to-soma transmission; Fig. 8).

Surprisingly, literature surveys reveal that germline invasion of endosymbionts from the soma every generation is the most common form of vertical inheritance (Russell *et al.* 2019). Vertical transmission via a continuous presence in the germline is much less common. One explanation is that hosts maintain mechanisms preventing endosymbiont occupation during the formative stages of germline development. In instances in which the endosymbiont is maintained in the germline, this may evolve into an obligate relationship in which development of the germline depends on the presence of the endosymbiont (Sullivan 2017). Examples of this include the leafhopper (*Euscelis plebejus*), in which the endosymbiont is required for normal embryonic development (Sander 1968). In addition, removal of *Wolbachia* from some insects results in increased apoptosis and abnormal oocyte development (Dedeine *et al.* 2001; Pannebakker *et al.* 2007). Here, we find that *Wolbachia* exhibit evidence of both the soma-to-germline and germline-to-germline transmission strategies (Fig. 8), suggesting that *Wolbachia* may stand out as a rarity among endosymbionts.

Data availability

Newly generated genomic data are available on GenBank (BioProject PRJNA907328). All other data are publicly available at figshare: https://doi.org/10.25386/genetics.22233817.

Supplemental material available at GENETICS online.

Acknowledgements

We thank Dr. Benjamin Abrams (UCSC Life Sciences Microscopy Center, RRID: SCR_021135) for his technical support and assistance with microscopy experiments. We thank Dr. Shelbi Russell for their helpful advice on imaging protocols and analysis. We thank Dr. Irene Newton for kindly supplying the anti-FtsZ antibody. We thank Will Conner for guidance with bioinformatic analyses and Tim Wheeler for laboratory assistance. We thank Drew Endy and the Free Genes Project for the gift of *Wolbachia* genes and advice on construction of pGH448. We are grateful for the feedback from 2 anonymous reviewers and the editor that improved the manuscript. We thank the Big Creek Reserve for use of their facilities. The microscopic analysis was enabled through the generous support of the IBSC microscopy facility at UC Santa Cruz.

Funding

Research reported in this publication was supported by the National Institute of General Medical Sciences of the National Institutes of Health under Award Number R35GM139595 to WS and R35GM124701 to BSC. This work was also supported by National Science Foundation (NSF) grants to WS (1456535) and BSC (2145195).

Conflicts of interest

The author(s) declare no conflict of interest.

Literature cited

Baldridge GD, Li YG, Witthuhn BA, Higgins L, Markowski TW, Baldridge AS, Fallon AM. Mosaic composition of ribA and wspB genes flanking the virB8-D4 operon in the *Wolbachia* supergroup B-strain, *w*Str. Arch Microbiol. 2016;198(1):53–69. doi:10.1007/s00203-015-1154-8.

Bastock R, St Johnston D. *Drosophila* oogenesis. Curr Biol. 2008;18(23):R1082–R1087. doi:10.1016/j.cub.2008.09.011.

Bilinski SM, Jaglarz MK, Tworzydlo W. The pole (germ) plasm in insect oocytes. In: Kubiak JZ, Kloc M, editors. Oocytes. Results and Problems in Cell Differentiation, vol 63. Cham: Springer; 2017. p. 103–126. doi:10.1007/978-3-319-60855-6_5.

Boettiger C, Coop G, Ralph P. Is your phylogeny informative? Measuring the power of comparative methods. Evolution. 2012;66(7):2240–2251. doi:10.1111/j.1558-5646.2011.01574.x.

Brendza RP, Serbus LR, Duffy JB, Saxton WM. A function for kinesin I in the posterior transport of oskar mRNA and Staufen protein. Science. 2000;289(5487):2120–2122. doi:10.1126/science.289.5487.2120.

Carrington LB, Lipkowitz JR, Hoffmann AA, Turelli M. A re-examination of *Wolbachia*-induced cytoplasmic incompatibility in California *Drosophila simulans*. PLoS One. 2011;6(7):e22565. doi:10.1371/journal.pone.0022565.

Casper-Lindley C, Kimura S, Saxton DS, Essaw Y, Simpson I, Tan V, Sullivan W. Rapid fluorescence-based screening for *Wolbachia* endosymbionts in *Drosophila* germ line and somatic tissues. Appl Environ Microbiol. 2011;77(14):4788–4794. doi:10.1128/AEM.00215-11.

Cha BJ, Koppetsch BS, Theurkauf WE. In vivo analysis of *Drosophila* bicoid mRNA localization reveals a novel microtubule-dependent axis specification pathway. Cell. 2001;106(1):35–46. doi:10.1016/s0092-8674(01)00419-6.

Cha BJ, Serbus LR, Koppetsch BS, Theurkauf WE. Kinesin I-dependent cortical exclusion restricts pole plasm to the oocyte posterior. Nat Cell Biol. 2002;4(8):592–598. doi:10.1038/ncb832.

Clark AG, Eisen MB, Smith DR, Bergman CM, Oliver B, Markow TA, Kaufman TC, Kellis M, Gelbart W, Iyer VN, *et al.* Evolution of genes and genomes on the Drosophila phylogeny. Nature. 2007;450-(7167):203–218. doi:10.1038/nature06341.

Cogni R, Ding SD, Pimentel AC, Day JP, Jiggins FM. *Wolbachia* reduces virus infection in a natural population of *Drosophila*. Commun Biol. 2021;4(1):1327. doi:10.1038/s42003-021-02838-z.

Conner WR, Delaney EK, Bronski MJ, Ginsberg PS, Wheeler TB, Richardson KM, Peckenpaugh B, Kim KJ, Watada M, Hoffmann AA, *et al.* A phylogeny for the *Drosophila* montium species group: a model clade for comparative analyses. Mol Phylogenet Evol. 2021;158:107061. doi:10.1016/j.ympev.2020.107061.

Conner WR, Blaxter ML, Anfora G, Ometto L, Rota-Stabelli O, Turelli M. Genome comparisons indicate recent transfer of *w*Ri-like *Wolbachia* between sister species *Drosophila suzukii* and *D. subpulchrella*. Ecol Evol. 2017;7(22):9391–9404. doi:10.1002/ece3.3449.

Cooper BS, Ginsberg PS, Turelli M, Matute DR. *Wolbachia* in the *Drosophila yakuba* complex: pervasive frequency variation and weak cytoplasmic incompatibility, but no apparent effect on reproductive isolation. Genetics. 2017;205(1):333–351. doi:10.1534/genetics.116.196238.

Cooper BS, Vanderpool D, Conner WR, Matute DR, Turelli M. *Wolbachia* acquisition by *Drosophila yakuba*-clade hosts and transfer of incompatibility loci between distantly related *Wolbachia*. Genetics. 2019;212(4):1399–1419. doi:10.1534/genetics.119.302349.

Cummings MR, Brown NM, King RC. The cytology of the vitellogenic stages of oogenesis in *Drosophila melanogaster*. 3. Formation of the vitelline membrane. Zellforsch Mikrosk Anat. 1971;118(4):482–492. doi:10.1007/BF00324615.

Dedeine F, Vavre F, Fleury F, Loppin B, Hochberg ME, Bouletreau M. Removing symbiotic *Wolbachia* bacteria specifically inhibits oogenesis in a parasitic wasp. Proc Natl Acad Sci U S A. 2001;98-(11):6247–6252. doi:10.1073/pnas.101304298.

Doyle MT, Bernstein HD. Bacterial outer membrane proteins assemble via asymmetric interactions with the BamA β-barrel. Nat Commun. 2019;10(1):3358. doi:10.1038/s41467-019-11230-9.

Ellegaard KM, Klasson L, Näslund K, Bourtzis K, Andersson SG. Comparative genomics of *Wolbachia* and the bacterial species concept. PLoS Genet. 2013;9(4):e1003381. doi:10.1371/journal.pgen.1003381.

Ferree PM, Frydman HM, Li JM, Cao J, Wieschaus E, Sullivan W. *Wolbachia* utilizes host microtubules and Dynein for anterior localization in the *Drosophila* oocyte. PLoS Pathog. 2005;1(2):e14. doi:10.1371/journal.ppat.0010014.

Fox DA, Larsson P, Lo RH, Kroncke BM, Kasson PM, Columbus L. Structure of the neisserial outer membrane protein Opa60: loop flexibility essential to receptor recognition and bacterial engulfment. J Am Chem Soc. 2014;136(28):9938–9946. doi:10.1021/ja503093y.

Fox J, Weisberg S. An R Companion to Applied Regression. Thousand Oaks (CA): SAGE; 2019.

Freckleton RP, Harvey PH, Pagel M. Phylogenetic analysis and comparative data: a test and review of evidence. Am Nat. 2002;160(6):712–726. doi:10.1086/343873.

Frydman HM, Li JM, Robson DN, Wieschaus E. Somatic stem cell niche tropism in *Wolbachia*. Nature. 2006;441(7092):509–512. doi:10.1038/nature04756.

Gabler F, Nam SZ, Till S, Mirdita M, Steinegger M, Söding J, Lupas AN, Alva V. Protein sequence analysis using the MPI bioinformatics toolkit. Curr Protoc Bioinformatics. 2020;72(1):e108. doi:10.1002/cpbi.108.

Gerth M, Bleidorn C. Comparative genomics provides a timeframe for *Wolbachia* evolution and exposes a recent biotin synthesis operon transfer. Nat Microbiol. 2016;2(3):16241. doi:10.1038/nmicrobiol.2016.241.

Grieder NC, de Cuevas M, Spradling AC. The fusome organizes the microtubule network during oocyte differentiation in *Drosophila*. Development. 2000;127(19):4253–4264. doi:10.1242/dev.127.19.4253.

Grobler Y, Yun CY, Kahler DJ, Bergman CM, Lee H, Oliver B, Lehmann R. Whole genome screen reveals a novel relationship between *Wolbachia* levels and *Drosophila* host translation. PLoS Pathog. 2018;14(11):e1007445. doi:10.1371/journal.ppat.1007445.

Guo Y, Gong JT, Mo PW, Huang HJ, Hong XY. *Wolbachia* localization during *Laodelphax striatellus* embryogenesis. J Insect Physiol. 2019;116:125–133. doi:10.1016/j.jinsphys.2019.05.006.

Hadfield SJ, Axton JM. Germ cells colonized by endosymbiotic bacteria. Nature. 1999;402(6761):482–482. doi:10.1038/45002.

Hague MTJ, Caldwell CN, Cooper BS. Pervasive effects of *Wolbachia* on host temperature preference. mBio. 2020b;11(5):e01768-20. doi:10.1128/mBio.01768-20.

Hague MTJ, Mavengere H, Matute DR, Cooper BS. Environmental and genetic contributions to imperfect *w*Mel-like *Wolbachia* transmission and frequency variation. Genetics. 2020a;215(4):1117–1132. doi:10.1534/genetics.120.303330.

Hague MTJ, Shropshire JD, Caldwell CN, Statz JP, Stanek KA, Conner WR, Cooper BS. Temperature effects on cellular host-microbe interactions explain continent-wide endosymbiont prevalence. Curr Biol. 2022;32(4):878–888.e8. doi:10.1016/j.cub.2021.11.065.

Hague MTJ, Woods HA, Cooper BS. Pervasive effects of Wolbachia on host activity. Biology Letters. 2021;17(5):20210052. doi:10.1098/rsbl.2021.0052.

Harmon LJ, Weir JT, Brock CD, Glor RE, Challenger W. GEIGER: investigating evolutionary radiations. Bioinformatics. 2008;24(1):129–131. doi:10.1093/bioinformatics/btm538.

Hilgenboecker K, Hammerstein P, Schlattmann P, Telschow A, Werren JH. How many species are infected with *Wolbachia*?—a statistical analysis of current data. FEMS Microbiol Lett. 2008;281(2):215–220. doi:10.1111/j.1574-6968.2008.01110.x.

Hoffmann AA, Turelli M, Harshman LG. Factors affecting the distribution of cytoplasmic incompatibility in *Drosophila simulans*. Genetics. 1990;126(4):933–948. doi:10.1093/genetics/126.4.933.

Höhna S, Landis MJ, Heath TA, Boussau B, Lartillot N, Moore BR, Huelsenbeck JP, Ronquist F. Revbayes: Bayesian phylogenetic inference using graphical models and an interactive model-specification language. Syst Biol. 2016;65(4):726–736. doi:10.1093/sysbio/syw021.

Hoskins RA, Carlson JW, Wan KH, Park S, Mendez I, Galle SE, Booth BW, Pfeiffer BD, George RA, Svirskas R The Release 6 reference sequence of the *Drosophila melanogaster* genome. Genome Res. 2015;25(3):445–458. doi:10.1101/gr.185579.114.

Hu TT, Eisen MB, Thornton KR, Andolfatto P. A second-generation assembly of the *Drosophila simulans* genome provides new insights into patterns of lineage-specific divergence. Genome Res. 2013;23(1):89–98. doi:10.1101/gr.141689.112.

Jackman SD, Vandervalk BP, Mohamadi H, Chu J, Yeo S, Hammond SA, Jahesh G, Khan H, Coombe L, Warren RL, *et al.* ABySS 2.0: resource-efficient assembly of large genomes using a Bloom filter. Genome Res. 2017;27(5):768–777. doi:10.1101/gr.214346.116.

Joshi N, Fass J. Sickle: a sliding-window, adaptive, quality-based trimming tool for FastQ files 2011.

Kamath AD, Deehan MA, Frydman HM. Polar cell fate stimulates *Wolbachia* intracellular growth. Development. 2018;145(6): dev158097. doi:10.1242/dev.158097.

Katoh K, Standley DM. MAFFT multiple sequence alignment software version 7: improvements in performance and usability. Mol Biol Evol. 2013;30(4):772–780. doi:10.1093/molbev/mst010.

Klasson L, Westberg J, Sapountzis P, Näslund K, Lutnaes Y, Darby AC, Veneti Z, Chen L, Braig HR, Garrett R, *et al.* The mosaic genome structure of the *Wolbachia wRi* strain infecting *Drosophila simulans*. Proc Natl Acad Sci U S A. 2009;106(14):5725–5730. doi:10.1073/pnas.0810753106.

Kose H, Karr TL. Organization of *Wolbachia* pipientis in the *Drosophila* fertilized egg and embryo revealed by an anti-*Wolbachia* monoclonal antibody. Mech Dev. 1995;51(2–3):275–288. doi:10.1016/0925-4773(95)00372-x.

Kühn S, Enninga J. The actin comet guides the way: how *Listeria* actin subversion has impacted cell biology, infection biology and structural biology. Cell Microbiol. 2020;22(4):e13190. doi:10.1111/cmi.13190.

Landmann F, Bain O, Martin C, Uni S, Taylor MJ, Sullivan W. Both asymmetric mitotic segregation and cell-to-cell invasion are required for stable germline transmission of *Wolbachia* in filarial nematodes. Biol Open. 2012;1(6):536–547. doi:10.1242/bio.2012737.

Luo Y, Ahmad E, Liu ST. MAD1: kinetochore receptors and catalytic mechanisms. Front Cell Dev Biol. 2018;6:51. doi:10.3389/fcell.2018.00051.

Mado K, Chekulayev V, Shevchuk I, Puurand M, Tepp K, Kaambre T. On the role of tubulin, plectin, desmin, and vimentin in the regulation of mitochondrial energy fluxes in muscle cells. Am J Physiol Cell Physiol. 2019;316(5):C657–C667. doi:10.1152/ajpcell.00303.2018.

Mahajan-Miklos S, Cooley L. Intercellular cytoplasm transport during *Drosophila* oogenesis. Dev Biol. 1994;165(2):336–351. doi:10.1006/dbio.1994.1257.

Maimon I, Gilboa L. Dissection and staining of *Drosophila* larval ovaries. J Vis Exp. 2011;(51): e2537. doi:10.3791/2537.

Meany MK, Conner WR, Richter SV, Bailey JA, Turelli M, Cooper BS. Loss of cytoplasmic incompatibility and minimal fecundity effects explain relatively low *Wolbachia* frequencies in *Drosophila mauritiana*. Evolution. 2019;73(6):1278–1295. doi:10.1111/evo.13745.

Merkle JA, Wittes J, Schüpbach T. Signaling between somatic follicle cells and the germline patterns the egg and embryo of *Drosophila*. Curr Top Dev Biol. 2020;140:55–86. doi:10.1016/bs.ctdb.2019.10.004.

Metcalf JA, Jo M, Bordenstein SR, Jaenike J. Recent genome reduction of *Wolbachia* in *Drosophila recens* targets phage WO and narrows candidates for reproductive parasitism. PeerJ. 2014;2:e529. doi:10.7717/peerj.529.

Noinaj N, Kuszak AJ, Gumbart JC, Lukacik P, Chang H, Easley NC, Lithgow T, Buchanan SK. Structural insight into the biogenesis of β-barrel membrane proteins. Nature. 2013;501(7467):385–390. doi:10.1038/nature12521.

O'Neill SL, Giordano R, Colbert AM, Karr TL, Robertson HM. 16S rRNA phylogenetic analysis of the bacterial endosymbionts associated with cytoplasmic incompatibility in insects. Proc Natl Acad Sci U S A. 1992;89(7):2699–2702. doi:10.1073/pnas.89.7.2699.

Pagel M. Inferring the historical patterns of biological evolution. Nature. 1999;401(6756):877–884. doi:10.1038/44766.

Pannebakker BA, Loppin B, Elemans CP, Humblot L, Vavre F. Parasitic inhibition of cell death facilitates symbiosis. Proc Natl Acad Sci U S A. 2007;104(1):213–215. doi:10.1073/pnas.0607845104.

Poinsot D, Bourtzis K, Markakis G, Savakis C, Merçot H. *Wolbachia* transfer from *Drosophila melanogaster* into *D. simulans*: host effect and cytoplasmic incompatibility relationships. Genetics. 1998;150(1):227–237. doi:10.1093/genetics/150.1.227.

Quinlan ME. Cytoplasmic streaming in the *Drosophila* oocyte. Annu Rev Cell Dev Biol. 2016;32(1):173–195. doi:10.1146/annurev-cellbio-111315-125416.

Ramalho MO, Vieira AS, Pereira MC, Moreau CS, Bueno OC. Transovarian transmission of *Blochmannia* and *Wolbachia* endosymbionts in the neotropical weaver ant *Camponotus textor* (Hymenoptera, Formicidae). Curr Microbiol. 2018;75(7):866–873. doi:10.1007/s00284-018-1459-3.

Raychoudhury R, Baldo L, Oliveira DC, Werren JH. Modes of acquisition of *Wolbachia*: horizontal transfer, hybrid introgression, and codivergence in the *Nasonia* species complex. Evolution. 2009;63(1):165–183. doi:10.1111/j.1558-5646.2008.00533.x.

Rice DW, Sheehan KB, Newton IL. Large-scale identification of *Wolbachia pipientis* effectors. Genome Biol Evol. 2017;9(7):1925–1937. doi:10.1093/gbe/evx139.

Rørth P. Initiating and guiding migration: lessons from border cells. Trends Cell Biol. 2002;12(7):325–331. doi:10.1016/s0962-8924(02)02311-5.

Ros, MD, Winston F, Hieter P. 1990. Methods in Yeast Genetics: A Laboratory Course Manual. Cold Spring Harbor, NY: Cold Spring Harbor Laboratory Press.

Russell SL, Chappell L, Sullivan W. A symbiont's guide to the germline. In: Lehmann R, editor. The Immortal Germline, Current Topics in Developmental Biology, vol 135. Academic Press; 2019. p. 315–351. doi:10.1016/bs.ctdb.2019.04.007.

Russell SL, Lemseffer N, Sullivan WT. *Wolbachia* and host germline components compete for kinesin-mediated transport to the posterior pole of the *Drosophila* oocyte. PLoS Pathog. 2018;14(8):e1007216. doi:10.1371/journal.ppat.1007216.

Salzberg SL, Dunning Hotopp JC, Delcher AL, Pop M, Smith DR, Eisen MB, Nelson WC. Serendipitous discovery of *Wolbachia* genomes in multiple *Drosophila* species. Genome Biol. 2005;6(3):R23. doi:10.1186/gb-2005-6-3-r23.

Sander K. Developmental physiological studies on embryonal mycetoma *Euscelis plebejus* I. Removal of and abnormal combination of unicellular components of symbiotic sysems. Dev Biol. 1968;17(1):16–38. doi:10.1016/0012-1606(68)90087-0.

Schrodinger LLC. The PyMOL molecular graphics system, version 1.8 2015.

Seemann T. Prokka: rapid prokaryotic genome annotation. Bioinformatics. 2014;30(14):2068–2069. doi:10.1093/bioinformatics/btu153.

Serbus LR, Casper-Lindley C, Landmann F, Sullivan W. The genetics and cell biology of *Wolbachia*-host interactions. Annu Rev Genet. 2008;42(1):683–707. doi:10.1146/annurev.genet.41.110306.130354.

Serbus LR, Cha BJ, Theurkauf WE, Saxton WM. Dynein and the actin cytoskeleton control kinesin-driven cytoplasmic streaming in *Drosophila* oocytes. Development. 2005;132(16):3743–3752. doi:10.1242/dev.01956.

Serbus LR, Ferreccio A, Zhukova M, McMorris CL, Kiseleva E, Sullivan W. A feedback loop between *Wolbachia* and the *Drosophila* gurken mRNP complex influences *Wolbachia* titer. J Cell Sci. 2011;124(24):4299–4308. doi:10.1242/jcs.092510.

Serbus LR, Sullivan W. A cellular basis for *Wolbachia* recruitment to the host germline. PLoS Pathog. 2007;3(12):e190. doi:10.1371/journal.ppat.0030190.

Serbus LR, White PM, Silva JP, Rabe A, Teixeira L, Albertson R, Sullivan W. The impact of host diet on *Wolbachia* titer in *Drosophila*. PLoS Pathog. 2015;11(3):e1004777. doi:10.1371/journal.ppat.1004777.

Sheehan KB, Martin M, Lesser CF, Isberg RR, Newton IL. Identification and characterization of a candidate *Wolbachia pipientis* type IV effector that interacts with the actin cytoskeleton. MBio. 2016;7(4):e00622-16. doi:10.1128/mBio.00622-16.

Steinhauer J, Kalderon D. Microtubule polarity and axis formation in the *Drosophila* oocyte. Dev Dyn. 2006;235(6):1455–1468. doi:10.1002/dvdy.20770.

Sullivan W. *Wolbachia*, bottled water, and the dark side of symbiosis. Mol Biol Cell. 2017;28(18):2343–2346. doi:10.1091/mbc.E17-02-0132.

Sullivan W, Ashburner M, Hawley RS. Drosophila Protocols. Cold Spring Harbor, NY: Cold Spring Harbor Press; 2000.

Suvorov A, Kim BY, Wang J, Armstrong EE, Peede D, D'Agostino ERR, Price DK, Waddell P, Lang M, Courtier-Orgogozo V Widespread introgression across a phylogeny of 155 *Drosophila* genomes. Curr Biol. 2022;32(1):111–123.e5. doi:10.1016/j.cub.2021.10.052.

Teufel F, Almagro Armenteros JJ, Johansen AR, Gíslason MH, Pihl SI, Tsirigos KD, Winther O, Brunak S, von Heijne G, Nielsen H. Signalp 6.0 predicts all five types of signal peptides using protein language models. Nat Biotechnol. 2022;40(7):1023–1025. doi:10.1038/s41587-021-01156-3.

Theurkauf WE. Microtubules and cytoplasm organization during *Drosophila* oogenesis. Dev Biol. 1994;165(2):352–360. doi:10.1006/dbio.1994.1258.

Theurkauf WE, Hazelrigg TI. In vivo analyses of cytoplasmic transport and cytoskeletal organization during *Drosophila* oogenesis: characterization of a multi-step anterior localization pathway. Development. 1998;125(18):3655–3666. doi:10.1242/dev.125.18.3655.

Theurkauf WE, Smiley S, Wong ML, Alberts BM. Reorganization of the cytoskeleton during *Drosophila* oogenesis: implications for axis specification and intercellular transport. Development. 1992;115(4):923–936. doi:10.1242/dev.115.4.923.

Toomey ME, Panaram K, Fast EM, Beatty C, Frydman HM. Evolutionarily conserved *Wolbachia*-encoded factors control pattern of stem-cell niche tropism in *Drosophila* ovaries and favor infection. Proc Natl Acad Sci U S A. 2013;110(26):10788–10793. doi:10.1073/pnas.1301524110.

Turelli M, Cooper BS, Richardson KM, Ginsberg PS, Peckenpaugh B, Antelope CX, Kim KJ, May MR, Abrieux A, Wilson DA Rapid global spread of *w*Ri-like *Wolbachia* across multiple *Drosophila*. Curr Biol. 2018;28(6):963–971.e8. doi:10.1016/j.cub.2018.02.015.

Turelli M, Hoffmann AA. Cytoplasmic incompatibility in *Drosophila simulans*: dynamics and parameter estimates from natural populations. Genetics. 1995;140(4):1319–1338. doi:10.1093/genetics/140.4.1319.

Veneti Z, Clark ME, Karr TL, Savakis C, Bourtzis K. Heads or tails: host-parasite interactions in the *Drosophila-Wolbachia* system. Appl Environ Microbiol. 2004;70(9):5366–5372. doi:10.1128/AEM.70.9.5366-5372.2004.

Weinert LA, Araujo-Jnr EV, Ahmed MZ, Welch JJ. The incidence of bacterial endosymbionts in terrestrial arthropods. Proc Royal Soc B. 2015;282(1807):20150249. doi:10.1098/rspb.2015.0249.

Werren JH, Baldo L, Clark ME. *Wolbachia*: master manipulators of invertebrate biology. Nat Rev Microbiol. 2008;6(10):741–751. doi:10.1038/nrmicro1969.

White PM, Pietri JE, Debec A, Russell S, Patel B, Sullivan W. Mechanisms of horizontal cell-to-cell transfer of *Wolbachia* spp. in *Drosophila melanogaster*. Appl Environ Microbiol. 2017a;83(7):e03425-16. doi:10.1128/AEM.03425-16.

White PM, Serbus LR, Debec A, Codina A, Bray W, Guichet A, Lokey RS, Sullivan W. Reliance of *Wolbachia* on high rates of host proteolysis revealed by a genome-wide RNAi screen of *Drosophila* cells. Genetics. 2017b;205(4):1473–1488. doi:10.1534/genetics.116.198903.

Wu M, Sun LV, Vamathevan J, Riegler M, Deboy R, Brownlie JC, McGraw EA, Martin W, Esser C, Ahmadinejad N, *et al.* Phylogenomics of the reproductive parasite *Wolbachia* pipientis *w*Mel: a streamlined genome overrun by mobile genetic elements. PLoS Biol. 2004;2(3):E69. doi:10.1371/journal.pbio.0020069.

Yang J, Zhang Y. I-TASSER server: new development for protein structure and function predictions. Nucleic Acids Res. 2015;43-(W1):W174–W181. doi:10.1093/nar/gkv342.

Zhang C, Freddolino PL, Zhang Y. COFACTOR: improved protein function prediction by combining structure, sequence and protein–protein interaction information. Nucleic Acids Res. 2017;45-(W1):W291–W299. doi:10.1093/nar/gkx366.

Zimmermann L, Stephens A, Nam SZ, Rau D, Kübler J, Lozajic M, Gabler F, Söding J, Lupas AN, Alva V. A completely reimplemented MPI bioinformatics toolkit with a new HHpred server at its core. J Mol Biol. 2018;430(15):2237–2243. doi:10.1016/j.jmb.2017.12.007.

Zug R, Hammerstein P. Still a host of hosts for Wolbachia: analysis of recent data suggests that 40% of terrestrial arthropod species are infected. PLoS One. 2012;7(6):e38544. doi:10.1371/journal.pone.0038544.

Editor: D. Barbash